Strategic Synthetic Color Tuning of Oxadiazole Based Luminescent Organoboron Compounds

A THESIS

SUBMITTED TO THE FACULTY OF THE GRADUATE SCHOOL

OF THE UNIVERSITY OF MINNESOTA

BY

Justin Wayne Hines

IN PARTIAL FULFILLMENT OF THE REQUIREMENTS

FOR THE DEGREE OF

MASTER OF SCIENCE

Prof. Paul Kiprof Adviser

May 2017

Acknowledgements

I would first like to thank my advisor, Dr. Paul Kiprof, for his research support and mentorship of the past two years. Much of what I have accomplished here at UMD is due to his guidance and I greatly appreciate the time spent working in his lab and all I have learned from him. I would also like to thank Dr. Venkatram Mereddy and Dr. Peter Grundt for teaching me the tactics and fineness required for organic chemistry, as well as the Mereddy group for their friendship and insights. In addition I would like to thank Kevin Wielenberg, whom was invaluable assisting in the lab, and Brian Gute and Romesh Lakhan who instructed me how to be an effective teacher. Finally I would like to thank Cole Holestrom for his assistance with all the instrumentation for this project, his support, and his friendship.

I dedicate this to my wife Jessica and my children, Dallas and Shanty for their love and support which made this achievement possible. I also dedicate this to my grandfather, Miles, may he rest in peace knowing I fulfilled his lifelong dream.

Abstract

Many organic dopants have been created for use in SMOLED displays, but few are composed of a family of compounds that spans large portions of the visible spectrum. Through careful design, a small family of simple oxadiazole based tetra-coordinated organoboron compounds of the type B(N,O)X has been developed with emission that spans the visible spectrum from violet to green. Oxadiazole based ligands were designed and utilized for their potential for heteroatomic substitution as well as their excellent electron transport properties. Significant changes in fluorescence were observed based on the isomeric substitution of the naphthalene substituent. Minimal bathochromic emission shifts were observed when the oxadiazole ligand was chelated with BPh_2, as well as minimal hypsochromic shifts when chelated to BF_2. This evidence suggests the emission of the complex is affected by the isomeric position and subsequent resonance of the oxadiazole ligand. Boron clearly forms a dative bond with the lone pair from the nitrogen on the oxadiazole ring. The data shows that this coordination is susceptible to hydrolysis even with the addition of hydrophobic phenyl groups, due to the oxadiazole ring's inherent electron deficiency and affinity for hydrogen bonding. This is evident especially in the boron trifluoride complex, in which the LCMS data shows the presence of only one fluoride atom.

Table of Contents

List of Figures

List of Tables

List of Schemes

Abbreviations

1,2 HPON	**2-(5-phenyl-1,3,4-oxadiazol-2-yl)naphthalen-1-ol**
2,3 HPON	**3-(5-phenyl-1,3,4-oxadiazol-2-yl)naphthalen-2-ol**
9BBN	**Banana Borane**
Alq3	**Aluminum Tris(8-Hydroxyquinolato)**
BODIPY	**Boron Dipyrrin**
DCM	**Dichloromethane**
DMF	**Dimethylformamide**
DMSO	**Dimethyl Sulfoxide**
EDG	**Electron Donating Group**
EML	**Emissive Materials Layer**
ETL	**Electron Transport Layer**
EWG	**Electron Withdrawing Group**
HOMO	**Highest Occupied Molecular Orbital**
HPOP	**2-(5-phenyl-1,3,4-oxadiazol-2-yl)phenol**
HTL	**Hole Transport Layer**
ITO	**Indium Tin Oxide**
LCD	**Liquid Crystal Display**
LCMS	**Liquid Chromatography Mass Spectroscopy**
LED	**Light Emitting Diode**
LUMO	**Lowest Unoccupied Molecular Orbital**
NMR	**Nuclear Magnetic Resonance Spectroscopy**

OLED	**Organic Light Emitting Diode**
OTf	**Triflate**
PHOLED	**Phosphorescent Light Emitting Diode**
PLED	**Polymeric Light Emitting Diode**
SMOLED	**Small Organic Light Emitting Diode**
THF	**Tetrahydrofuran**
TLC	**Thin Layer Chromatography**
UMD	**University of Minnesota-Duluth**
UV	**Ultra Violet**
UV-Vis	**Ultra Violet Visible Spectrum**

Aspects and overview

OLED technology has progressed greatly in recent years as the demand for flexible displays, wider color variety, and better picture quality has increased. The emissive materials themselves have been the primary focus of OLED research, as such numerous materials have been researched and designed for that purpose. Boron complexes and oxadiazoles have been used separately for organoluminescent materials, but little research has been done to explore a combination of their unique characteristics.

The bulk of current luminescent organoboron compounds and oxadiazole compounds were investigated in this paper. The materials researched were used in designing our own ligands for such emissive materials. A new family of organoluminescent oxadiazole boron complexes was designed with the overall goal of color tuning of the ligand. The scope of this thesis is divided into three chapters: research and design, rationalization of photophysical properties, and experimental. The development process of our luminescent compounds with respect to what is known about organoboron compounds as well as oxadiazole compounds in both present and past literature is covered in the first chapter of this paper. The second chapter covers the investigation into the oxadiazole based ligand, rationalization of luminescent properties and characterization of structural influences on color tuning by use of NMR, UV-Vis, and LC-MS is presented. Finally, details of experiments and procedures used are outlined in the third chapter.

Chapter 1

The History and Application of Boron

Boron was originally discovered in 1808 by Sir Humphry Davy, Joseph Louis Gay-Lussac, and Louis Jacques Thenard. Davy termed the element boracium however it was not officially discovered and recognized until 1828 by Jons Jako Berzelius. It wasn't until 1909 that the American chemist produced boron in its elemental form. [1,2]

Boron is fairly rare, making up only .001% of the earth's elemental mass. The majority of boron containing ore deposits are found in Turkey, with the second largest deposit residing in the United States. [3] The most common use for boron, by mass, is the production of borosilicate glass from B_2O_3.[4,5] Boron is extracted from naturally occurring minerals, such as kernite and borax, and converted into boric acid. Pure boron is derived from BBr_3 under extreme conditions with H_2, but is difficult due to impurities from carbon and various other trace elements.[5]

Boron is widely used in industry and scientific research. It has applications ranging from synthetic chemistry, medicinal uses, material science, and manufacturing. Since the discovery of hydroboration, boron has been a cornerstone of organic chemistry.[6] After the first borohydride reagent with significant synthetic applications was discovered by Brown and Krishnamurthy, hundreds of boron reagents have been developed. Many of the reagents used today were developed by Brown himself.[6,7] After the naturally occurring alpha pinene's properties as a chiral auxiliary for hydroboration were discovered, it has been used for a wide range of reactions including but not limited to reduction, hydroboration, homologation, enolboration, epoxide ring opening, and crotylboration all

of which are asymmetric and highly selective reactions **FIG 1**.[8,9] Even the simplest of boron reducing agents, sodium borohydride, can be coupled with a lanthanide to perform highly selective reductions of alpha enones. This is more commonly referred to as Luche Reduction.[10] Possibly the most famous and most widely used boron reaction is the C-C bond forming reaction known as Suzuki Coupling. With carefully designed palladium catalysts, the sp^2-sp^2 and sp^2-sp^3 carbon bond forming reactions that were previously impossible can almost indefinitely be achieved.[11] The sheer number of synthetic applications are too numerous and too broad in their potential applications to cover.

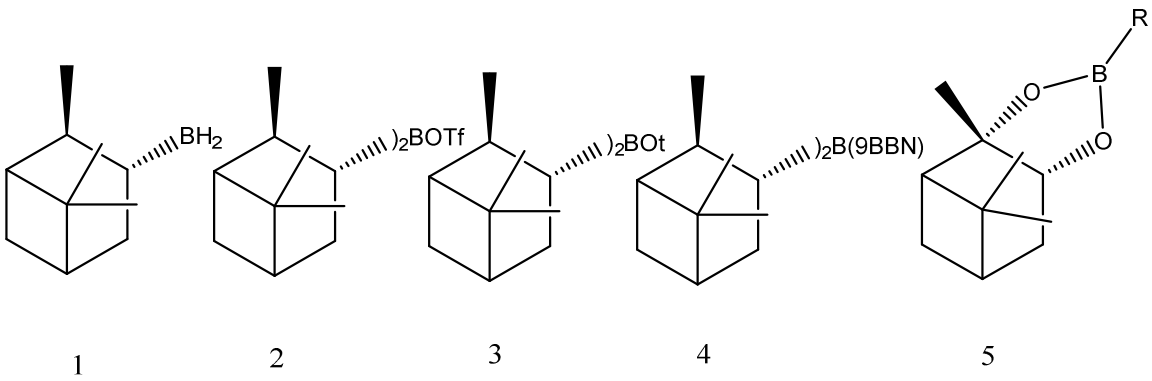

Fig 1 Common chiral alpha pinene derivatives for use in asymetric hydroboration (**1,4)**, asymmetric tosylation (**2**), asymmetric crotylation (**3**), and asymmetric homologation (**5**)

The medical applications of boron are well documented with new research broadening its uses every day. New research into benzoboroxole derivatives has shown they exhibit antibiotic,[12] antifungal,[13] antimalarial,[14] and antiprotozoal[15] drugs **FIG 2**. Boron has been successfully used as an anticancer treatment in the form of B-10.[16] This particular treatment is highly selective but has shown difficulty in the delivery of the treatment compounds to the affected areas in the necessary concentrations.[16]

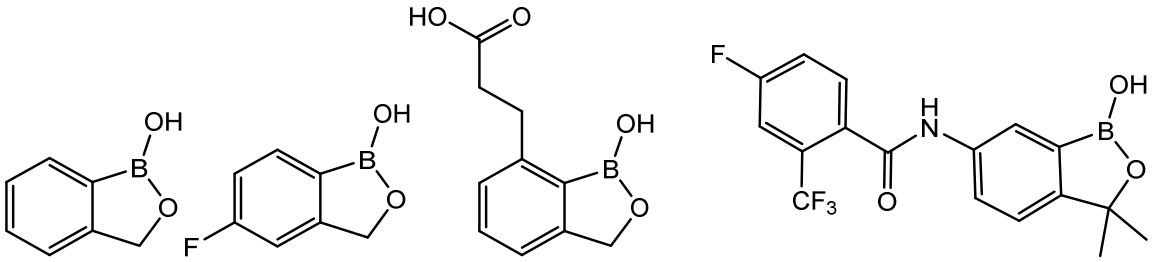

FIG 2 Biologically active benzoboroxoles for use in antibiotics (**1,2**),[12] antifungals (**2**),[12,13] antimalarial (**3**),[14] and antiprotozoal (**4**)[15] drugs.

In recent literature, boron has been incorporated and or materials designed around its implementation in light harvesting photovoltaics,[17,18] molecular switches,[19,20] lasing dyes,[21] non-linear optics,[22,23] biomolecular probes,[24,25] chemosensors,[26] energy transfer cassettes,[27] and superconductors.[28,29]

The majority of boron based chemosensors share many structural traits to boron based OLED materials,[26,30-32] Generally they manipulate the same properties of boron, namely its empty p_z orbital and natural Lewis acid character. Luminescent organoboron compounds are highly sensitive to the coordination and electronic environment of the boron, relying primarily on the conjugation of the system and the pπ-pπ* interactions across boron's empty orbital.[33] Three coordinate boron systems readily form dative bonds with strong electron donors such as fluorine, which drastically alter the overall luminescent properties of the compound.[26,31-34]

Characteristics and Applications of Oxadiazole Compounds

Oxadiazoles are five membered heterocyclic compounds in the azole family, with three stable isomers. The 1,2,4-isomer 1,3,5-isomer and 1,3,4-isomer are stable, however the

1,2,3-isomer undergoes ring opening forming the more stable diazoketone tautomer **FIG 3**.[35]

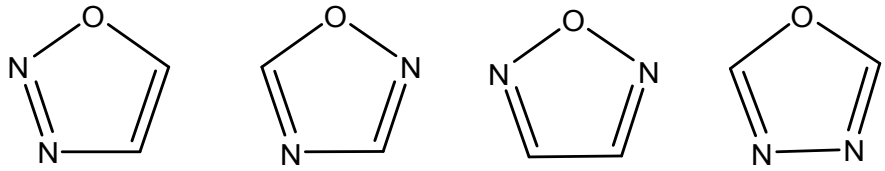

1 2 3 4

FIG 3 The 1,2,3-oxadiazole isomer (**1**), 1,2,4-oxadiazole isomer (**2**), 1,2,4-oxadiazole isomer (**3**), and the 1,3,4-oxadiazole isomer(**4**).

Oxadiazoles are inherently electron deficient overall, yet the nitrogen atoms show Lewis base characteristics similar to pyridine. These properties have been used with great success in biomedical and material science applications.

A wide array of oxadiazole compounds have medicinal applications including antifungal,[36] antibacterial,[37-39] antimicrobial,[37-43] antiviral,[45] anti-HIV,[46] antitubercular,[40,48] and anticancer[43,45-49] pharmaceuticals with new research and applications occurring worldwide. The heterocyclic nature of the oxadiazole rings allow for high activity due to their ability to cross cell membranes efficiently allowing for easier uptake into targeted cells.[36-49]

Oxadiazoles are excellent for material science field of optics such as nonlinear optics and organic light emitting diodes due to their electron deficient nature.[50] NLO is a broad range of concepts and applications including data storage, optical communication, image transmission, signal processing, data storage, and optical computing while OLEDs are

used primarily for flat panel displays in televisions, laptops, and cellphones.[55-57] Oxadiazoles' electron deficient nature makes them excellent electron transport compounds and their luminescent properties can be easily tuned by modifying the compounds overall electronic environment.[50] This is typically done by extending the pi system of the compound, such as increasing the overall conjugation of the system, or by complexing the compound with a metal. Various metals have been used with oxadiazole based compounds to great effect FIG4.[50-54]

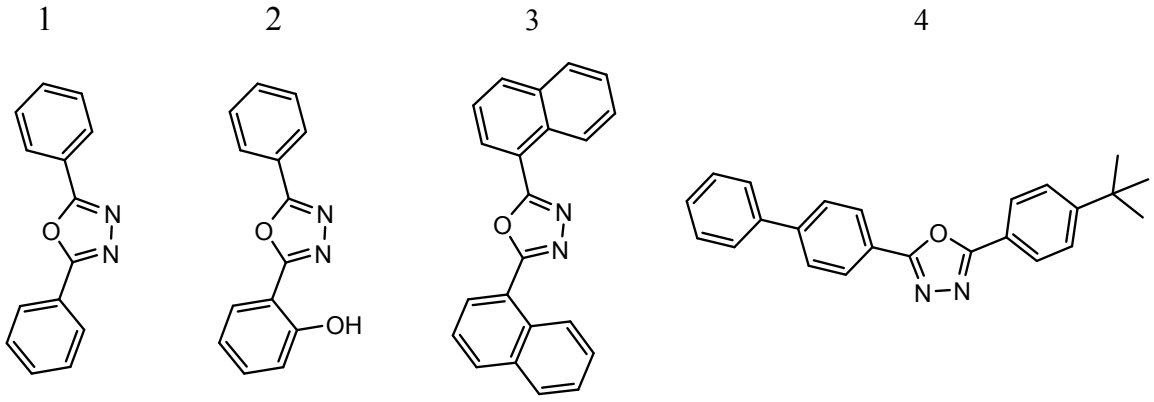

FIG 4 Various luminescent oxadiazole based compounds chelated with Iridium**(1)**[51], Aluminum**(2)**[50], Biphenyl Boron(**2**)[54], Cesium**(3)**[52], and Tin**(4)**[53] respectively.

Overview of LCD's and OLED's

Since the discovery and fabrication of the first practical OLED by Tang and Van Slyke using the Alq_3 complex,[58] a wide array of organic compounds and devices have been developed for their numerous advantages over modern LCD.[59,60]

The typical LCD display consists of two polarized filters and ITO electrodes that encapsulate the nematic liquid crystal. Incident light produced at the back of the device is circularly polarized by the liquid crystal, allowing it to pass through the horizontal filter. When a voltage is applied to the nematic crystal it straightens, there by turning off the pixel by keeping the light polarized vertically. The incident light is produced from a white backlit source while the color for each pixel is provided by an appropriately colored filter **FIG5**.[61]

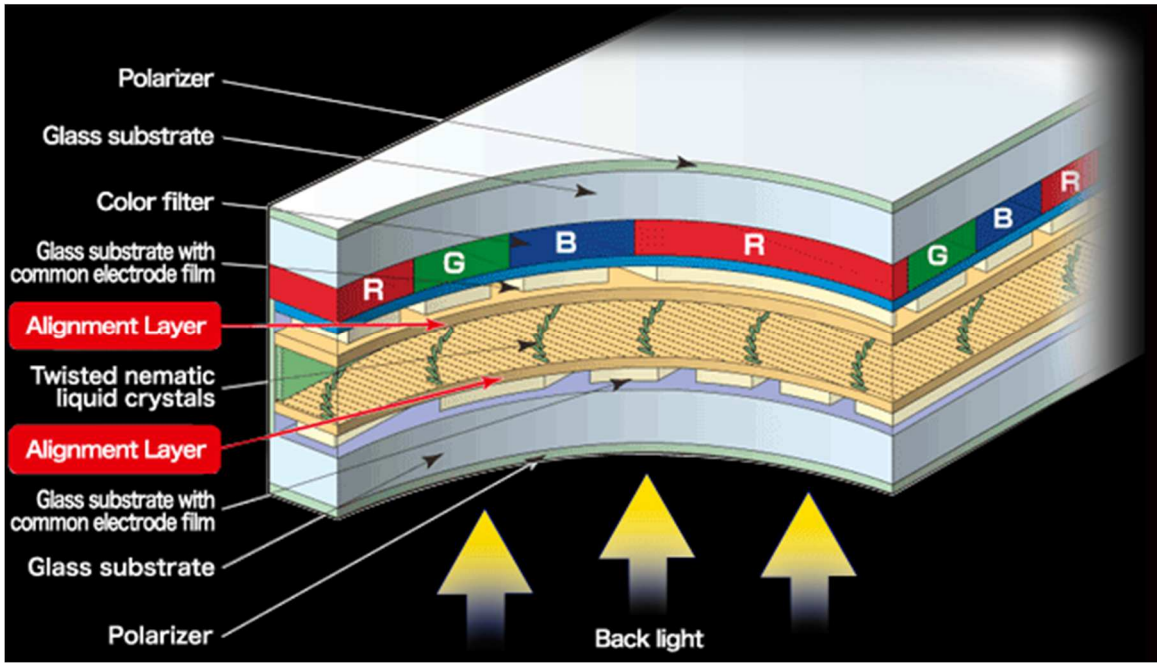

FIG 5 Basic LCD pixel cross-section.[62]

This design has severely limited its efficiency and applications. The LCD operates on absorbing light, however as light inevitably leaches through the polarized glass the realization of a true black pixel reduces total emissive luminescence and global contrast ratio. Also the action of straightening the twisted crystals can be slow which causes slower refresh rates and overall blurred images. Finally, the liquid crystal cell design

requires a rigid and thick structure when compared to an OLED. This prevents LCD's from various applications in which OLED's excel such as semiconducting thin films.[62]

OLED devices overcome many of the short comings of LCD's. Basic OLED's consist of three simple layers; electron transport layer, emissive material layer, and hole transport layer. These layers are contained between two ITO and alloy electrodes **FIG 6**. These layers are remarkably thin compared to an LCD, no more than 10nm each, which allows for thinner and lighter displays. Each of these layers are specifically designed to so that their semiconducting properties are compatible, in that the LUMO of the n-type ETL is nearly isoenergetic with the EML. Without this compatibility the overall efficiency of the device is drastically reduced to the resulting charge imbalance forcing the need for higher voltages to operate the device. These principles also apply to HOMO of the p-type semiconducting layer, or the hole transport layer. This design makes each OLED unique in its composition and how the individual layers coordinate. In some instances, based on composition and device architecture, additional layers may be required for optimum efficiency and functionality. These additional layers are typically hole transport blockers or electron blockers located next to the EML to prevent wide band gaps. Materials that function as semiconductors and emissive materials are highly desirable to decrease the number of layers needed for device function as well as reducing the exiplex emission resulting from the interactions between different materials at their interface.[59,60,63-65]

By design, OLED's are operationally simplistic. Charges are injected in the HTL and ETL **FIG 7**. Physicists commonly refer to these quasiparticles as polarons. This is achieved by injecting electrons into the LUMO of the ETL or removing electrons from

the HTL. These polarons are driven by the applied voltage at the electrodes and as the device is operated these polarons travel, or "hop" through the layers of the OLED to the EML. Once they reach the EML they recombine resulting in photonic emission from the device by charge recombination, unlike fluorescence which is typically a result of electronic relaxation.[59,60,63-65] The wave length of the emission corresponds to the fluorescence band gap of the EML used.

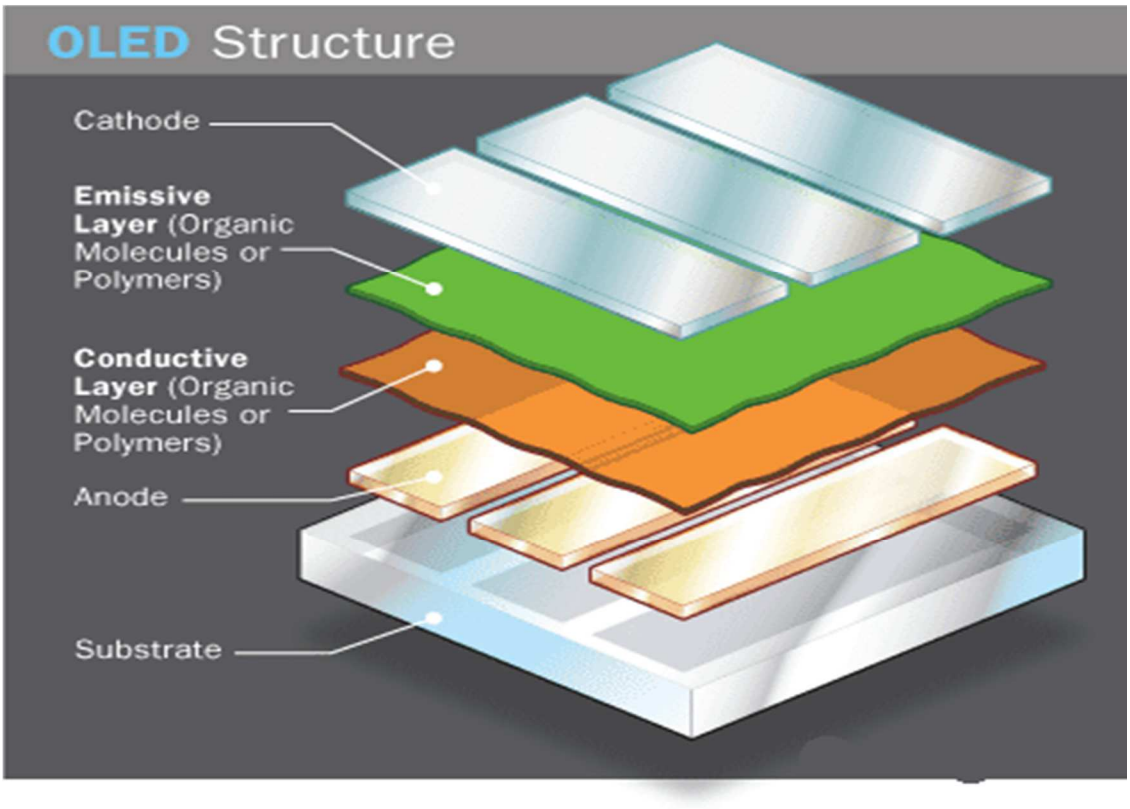

FIG 6 The structure of a simple OLED[66]

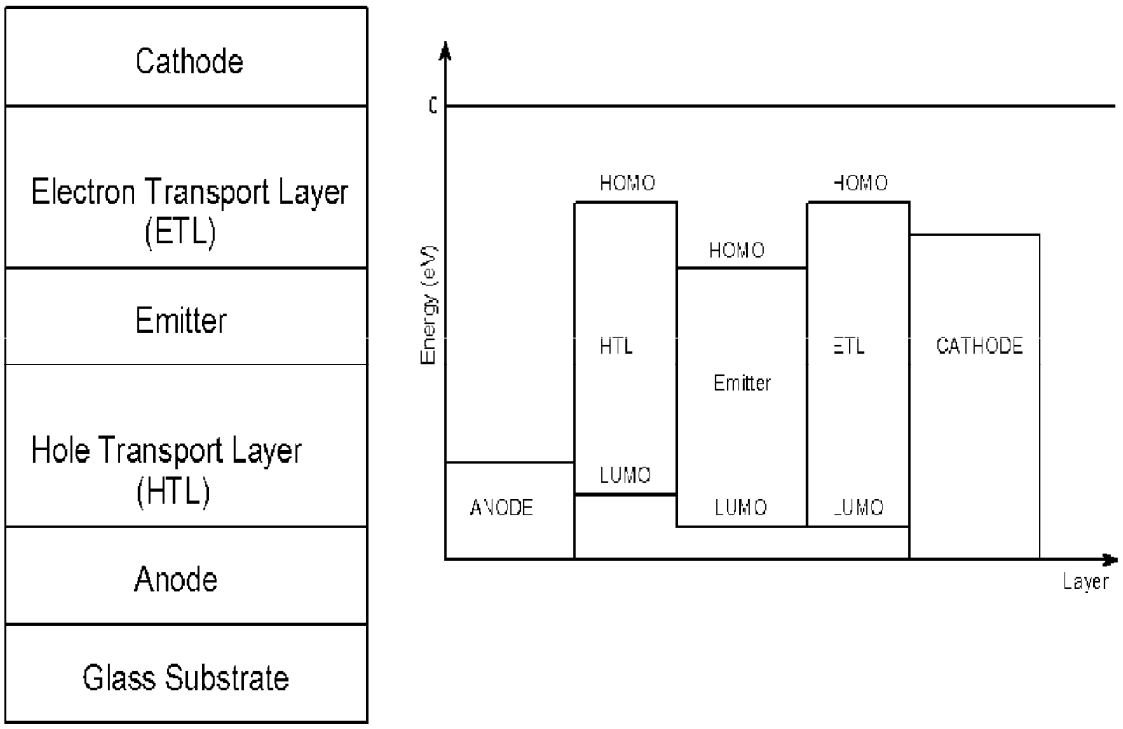

FIG 7 The relative energy states of the individual layers of a basic OLED[66].

Based on the broad range of semi-conducting materials available and wide variety of fabrication methods OLED's can range from flexible electronic displays to solid state lighting. Depending on the materials and fabrication methods used OLED's typically fall into one of three categories: SMOLED, PLED, and PHOLED. From a fabrication and manufacturing stand point SMOLED's are more complex to produce because they rely on doping via vapor deposition. However, this allows for endless synthetic possibilities for creating new luminescent compounds. PLED devices are highly desirable because many of the oligomeric chains are semi-conductive, allowing for less layers in the device. Additionally, these polymer chains can easily be synthesized and fabricated into flexible displays that are currently in high demand. PHOLEDs are a combination of SMOLEDs and PLEDs, however the EML is comprised of a phosphorescent material instead of

fluorescent material. Due to the spin rules of phosphorescent charge combination, emissions near quantum unity can be achieved.[63-65]

By design, OLEDs overcome many of the limitations of LCDs. Since the OLED operates based on emission instead of absorption it is over all more energy efficient by eliminating the need for a constant back light. They also can achieve a true black, which is another major limitation in LCD devices. Because of the switch nature of OLED design it is able to achieve better refresh rates. The wide array of OLED designs and composition allows for higher chromaticity, contrast ratios, luminosity, as well as display size and flexability.[63-65]

OLEDs do have certain limitations. Currently many have issues with low melting points which cause the pixel to short out, moisture sensitivity leading to layer degradation, and blue emissive materials have short lifetimes. Yet the sheer amount of potential material design, architecture, and groundbreaking research insures that OLEDs will surpass current LCD's in the near future.[59,60,63-65]

This information is only a brief overview of OLED and LCD technology. There is a massive collection of data and publications revolving around these technologies with far more detailed information on their complex functionality and design.[59-65]

Boron and Oxadiazole Compounds for OLED Applications

As previously discussed, OLED devices rely on the π to π orbital interactions in the organic semi-conductors to undergo the charge "hop" mechanism. This necessitates the use of low band gap materials that are tunable for device fabrication. Based on these parameters many boron based chelates have been research as alternatives to the

predominant transition metal based compounds. Their chemical nature has allowed for the synthesis of many boron based emissive dopants that are easily tunable as EML type compounds.[66-73] Many of boron's unique chemical properties have fueled its application to OLED research. When in the ground state boron possesses three valence electrons, and when in the binding state an s orbital and two p orbitals are combined into the sp^2 hybridized trigonal planer geometry, while being two electrons short of an octet.[74] This causes boron to have a high ionization energy and covalent bond nature instead of the trivalent nature of other similar elements.[75] Donation of electron density into boron's empty p orbital can further shorten this covalent bond **FIG 8**.[74,76]

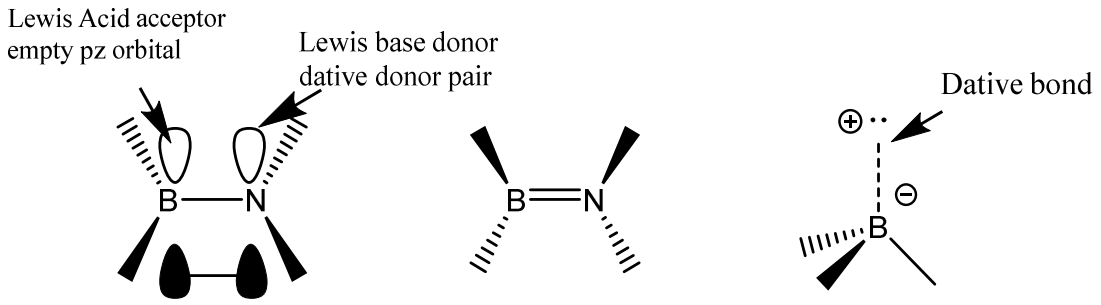

FIG 8 The Lewis acid base pairing of boron-nitride adducts results in shortening of the bond distance (**left**); tetrahedral hybridization of boron (**right**)

Boron's strong Lewis acidity stems from its empty p_z orbital, allowing it to readily accept two electrons through Lewis acid base pairing or dative bonding.[5,77] A vast array of organic chelates exploit this property for OLED applications due to its unique ability to form a tetrahedral geometry when bound with a dative bond, thus locking extended π systems into co-planarity for maximum π system overlap. This dative bonding is usually with N,N or N,O chelates. The dative bonds ability to pseudo extend the conjugated π system in this manner has been shown to enhance the photoluminescence of the

system.[78,66] Organoboron compounds are widely used as ETL for their ability to easily facilitate highly polarized charge transfer through boron's p_z orbital to π orbital interactions.[67]

Boron's covalent sigma bonding nature, due to its high charge density and small atomic size, provides many advantages over its group 13 counterpart, aluminum.[74] Boron compounds are more stable than their aluminum or zinc counterparts due to this covalent bonding.[79-82] Thus, many numerous boron based derivatives of the Alq_3 compound have been made[68-70,81,83-86], and these analogous boron compounds are what inspired our development of new organoboron luminescent compounds. As previously stated there are two main types of organoboron chelates; N,N type and N,O type.

Simple N,N type chelates are very popular presumably due to their easy chelation with boron and the long term stability of the resulting compounds. Arguably the most famous of these chelates the BODIPY dye and its numerous derivatives **FIG 9**.

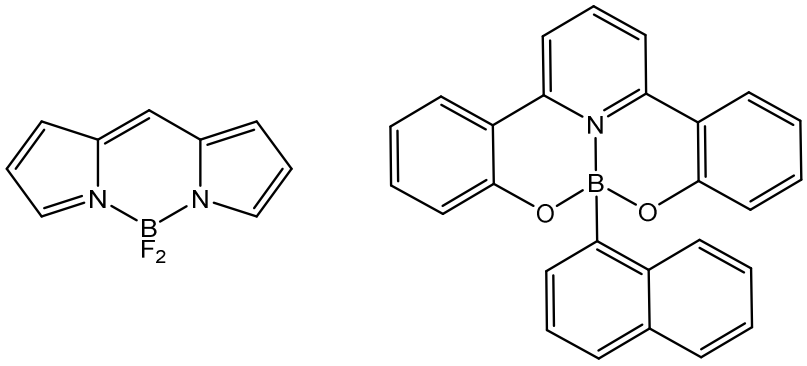

FIG 9 The core of the ubiquitous BODIPY dye(**right**)[87] and the basic scaffold of a closely related polydentate polypyridine dopant(**left**)[88,89]

There are numerous publications and reviews on BODIPY and its derivatives describing in detail various methods of color tuning. The use of BODIPY fluorophores in OLED's

however many tridentate compounds similar to the BODIPY core have been synthesized with OLED fabrication in mind.[71-73,83,90-92] The most numerous of these are based on the 2-pyridyl scaffold **FIG 10**. Small modifications to the 2-pyridyl scaffold have led to a wide variety of compounds with emission that span nearly all of the visible spectrum.[72,73] Further tuning of the emissions were achieved by fluorination of the scaffold, however the small changes in emission proved not to be cost effective based on the necessary materials and methods of synthesis.[72]

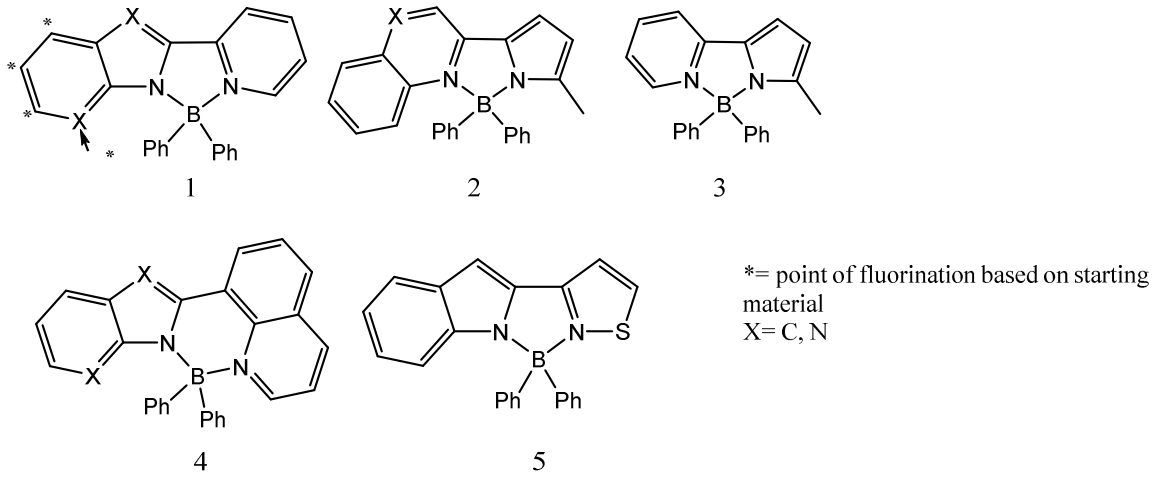

FIG 10 Examples of the 2-pyridyl scaffold derivatives.[72,73,91,92]

Since Tang and Van Slyke's synthesis of the aluminum tris-quinolate scaffold N,O-type chelates have become the most popular and widely researched chelate with respect to boron based OLED applications. Many of these BAr_q compounds have been synthesized as dopants for EML, however given their versatility many have been designed into emissive polymers[69,83] and even dual functioning multinuclear ETL-EML materials.[63] The two primary means of tuning the BAr_q compounds are extending the π conjugate system and the use of EDG or EWG substituted on the quinolate core.[65,66,85,86] Research has shown that extending the conjugate π system or using EDG causes the emissions to

shift bathochromatically.[70,85] The use of EWD causes the emissions to shift hypsochromatically[70,85] **FIG 11**.

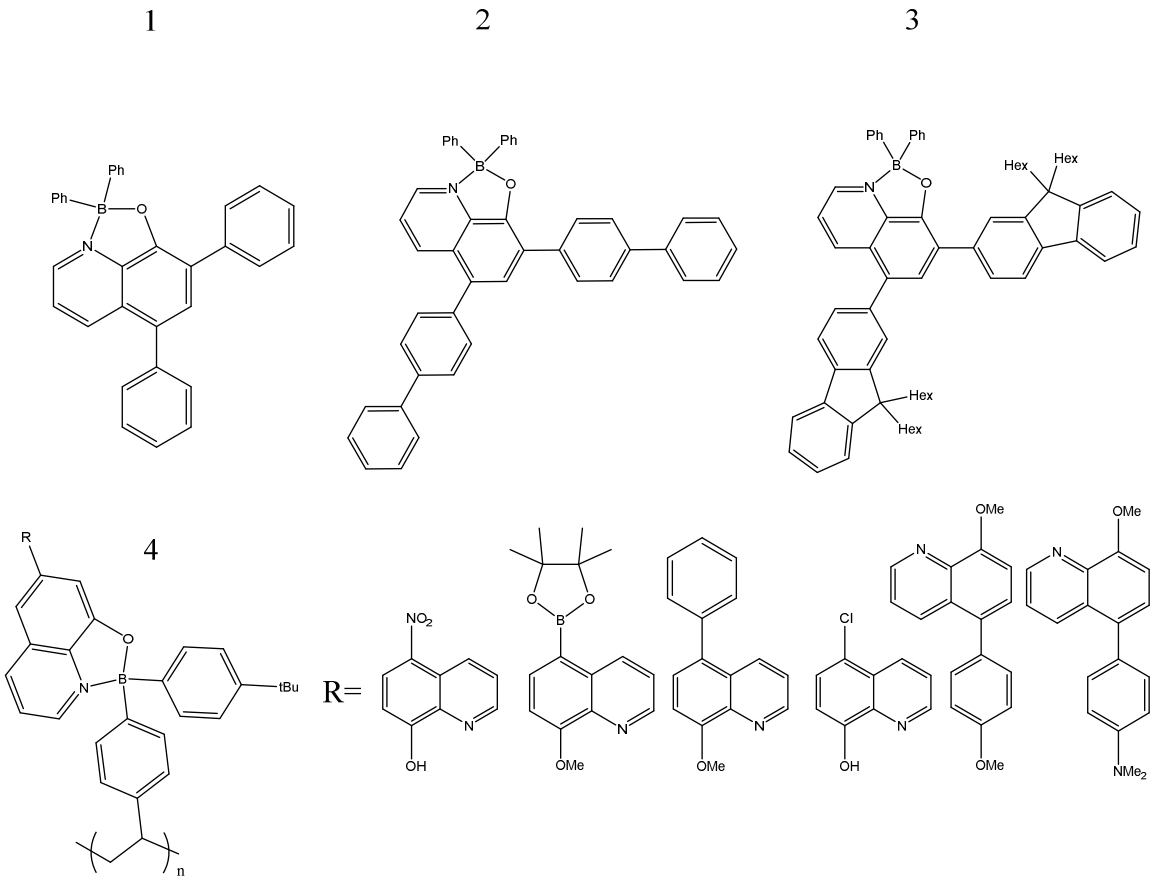

FIG 11 Tuning of the quinolato core through means of π conjugate extension **(1-3)**[85], and through the use of various EDGs and EWGs on a polymeric scaffold **(4)**[69].

Oxadiazoles are N,O-type ligands that have been recently studied for OLED applications. Tang and Van Slyke extended their previous work with aluminum trisquinolate by replacing the quinolate with an oxadiazole, which also formed a three coordinate structure. Research into this new oxadiazole ligand, HPOP, showed promising results for OLED applications when complexed with various metals **FIG 4**.[50]

These luminescent boron and oxadiazole based compounds have largely been the influence for new OLED materials in our lab. I have extensively researched both organoluminescent boron compounds as well as various oxadiazole compounds as a basis for designing a new family of ligands for boron based OLED materials. Rationalization of color tuning techniques have been successfully implemented from the literature in producing new oxadiazole ligands for boron fluorophores with OLED type material fabrication in mind.

Chapter 2

Synthesis and Development of New Boron-Oxadiazole Complexes

Our group's interest in organic luminescent compounds began with benzoboroxole, a heterocyclic polycycle that was first reported by Snyder in 1957.[93] Benzoboroxole consists of an aromatic six membered ring and a boron containing five membered heterocycle. Shortly after its discovery, it was researched for its unique synthetic characteristics and material applications.[94-96] Benzoboroxole derivatives have been used for antibiotic, antifungal, antimalarial, antiprotozoal pharmaceuticals, glycoconjugates, Suzuki coupling, blue dyes, plastic biocides, and OLED materials.[12-15,96] Recently colleagues in Dr. Mereddy's lab found a simple reaction to synthesize benzoboroxole with consistent yields of 80 percent or more by reduction with sodium borohydride of the corresponding 1,2-type substituted boronic acid-aldehyde **Scheme 1**.

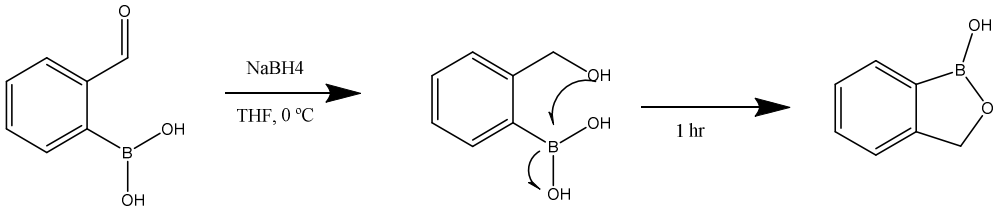

Scheme 1 Synthetic route to benzoboroxole through reduction using sodium borohydride.

With the improved synthesis method, many research groups at UMD sought out new uses for the benzoboroxole family. It was soon discovered that benzoboroxoles, like other boron adducts, can be condensed with N,O-type ligands to form organoluminescent compounds.[96] This condensation uses boron's Lewis acidity to exploit boronic acids

ability to form boronic esters rapidly and reversibly with either primary or secondary alcohols **Scheme2**.[97]

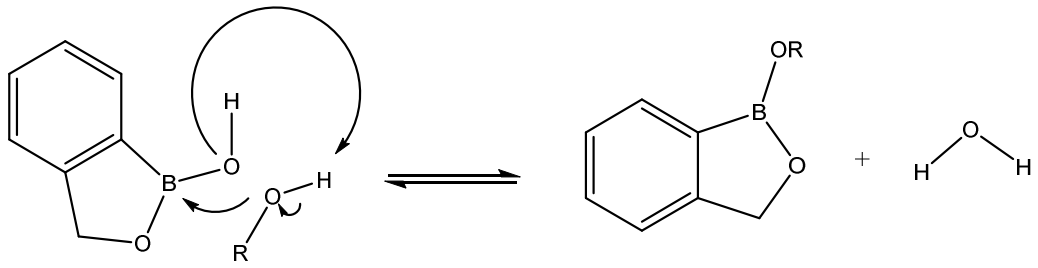

Scheme 2 Proposed mechanism of condensation in formation of boron esters.

When benzoboroxole was condensed with 8-hydroquinolate, and more recently 10-hydroquinolate it formed emissive compounds analogous to Tang's Alq_3.[98] Another compound analogous to Tang's Alq_3, $Al(POP)_3$ showed significant results in fluorescence in the blue range, thus our research into combining the emissive properties of benzoboroxole with the tuning capabilities shown in oxadiazoles began.[50]

We started by extending the π conjugate system of the oxadiazole by using the 1,2-naphthalene and 2,3-naphthalene analog of the HPOP ligand because of its proven success coordinating to various metals as well as biphenyl boron.[50-54] The first ligand we studied was the 1,2 HPON, which proved difficult to synthesize due to impurities during several of the steps. The addition of the hydrazide functional group proved to be the most difficult, with the lowest yield of pure products **Scheme3**. The most problematic step proved to be the hydrazide addition. The original synthetic method of refluxing the solution yielded no product as well as no starting material. The H^1NMR showed the formation of the carboxylic acid. We then attempted to use the acid chloride derivative, however the synthesis of the acid chloride yielded many impurities and low overall

yields. When the hydrazide addition was attempted, the product was an insoluble dimer with naphthalene groups on each side. Then the original synthesis method was revisited under the assumption that the refluxing process caused the hydrazine to evaporate before the reaction could occur, despite the condenser apparatus. When mildly heated to 70º C the reaction formed the desired product, however the yields were unreliable. It consistently had a yield of 100% or more and the H^1NMR showed a rapid hydrogen transfer from residual water to the primary amine. There were many attempts to remedy this occurrence, the used of desiccant in the condenser, molecular sieves in the solution, drying in vacuo, recrystallization from various dry solvents, and even air drying. None of these procedures removed the residual water, and the last two procedures actually increased the water in the product. However, this residual water did not affect later reactions although the following step's yield calculation was skewed. Synthesis of the 2,3-HPON was much more efficient with higher yields and minimal purification required.

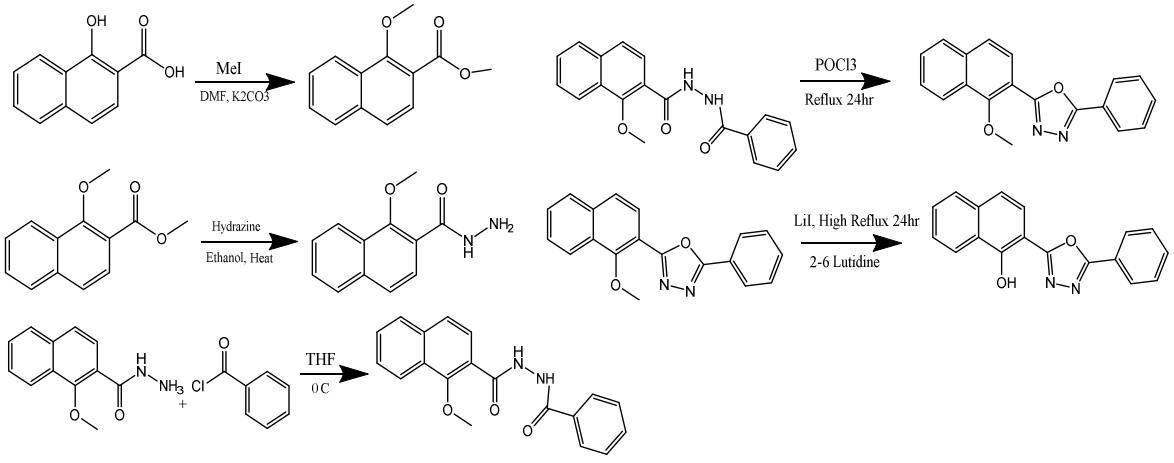

Scheme 3 Synthesis of 1,2-HPON Ligand, 2,3 HPON ligand follows the same scheme

We then attempted to tune the emissions with EDG and EWD in the 4 position of the benzoboroxole's six membered aromatic ring. Ultimately the benzoboroxoles did not

chelate with either of the oxadiazole derivatives **Scheme4**. Many different synthesis methods were attempted to achieve product formation. All reactions were monitored by TLC. The first method was simple reflux in dry toluene. When this failed, the reaction temperature was increased and a Dean-Stark trap was used. However, the small amount of water produced by the condensation reversed the reaction to starting material too quickly to be removed during the reflux. Next, the reaction was attempted with molecular sieves in the reaction vessel as well as a Dean-Stark trap. The slight acidity of the molecular sieves decomposed the oxadiazole ring and prevented the desired product formation. Then we tried various hydrides to accelerate the reaction. This had the unintended effect of the respective hydride salt coordinating to the ligand instead of the boron compound. The rigid structure of the boron containing five membered heterocycle, reverse hydrolysis resulting in starting material, the electron repulsion of the oxygen heteroatom, its electron withdrawing effects, and the hydrophilic nature of the oxadiazole are all potential factors causing the unsuccessful chelation of the N,O-type ligand and the benzoboroxoles.

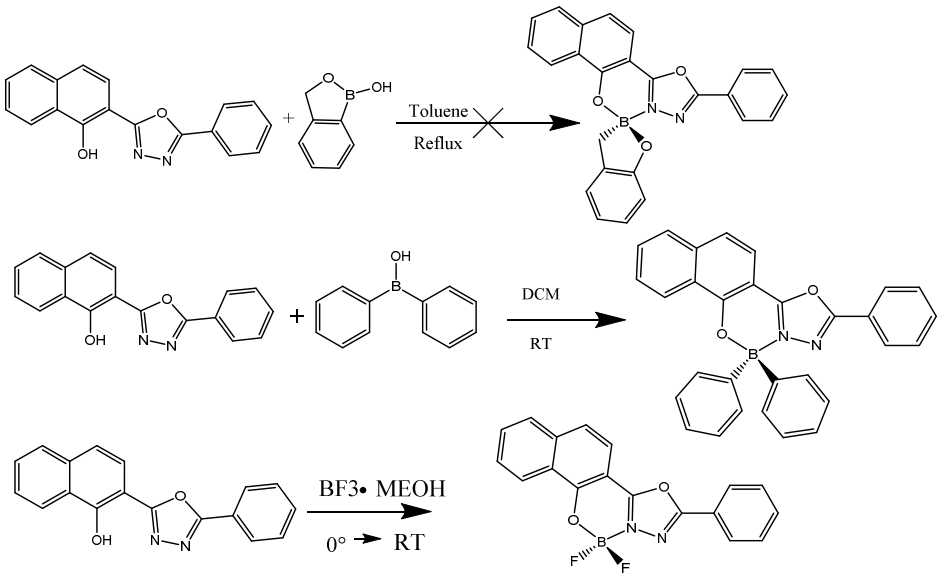

Scheme 4 Chelation of the oxadiazole ligand to the boron compounds

Thus we moved on to other boron containing compounds. Again we used boron compounds with EDG and EWD to tune the emissions. The synthesis of these complexes were much more simplistic and efficient. Originally the reactions were performed in THF at 0ºC and stirred to room temperature. This lead to a mixture of products and a yield of 15% after purification. This is presumably due to the presence of moisture in the THF. Next the reactions were run in DCM under the same conditions. Again, there were similar results, presumably from high humidity or condensation accumulating inside the flask. Finally the reaction was run in dry DCM at room temperature and stirred. Product formation occurred in approximately 30 seconds by crashing out of solution. The reaction was also observed under a UV light. This synthesis method had a yield of 80-90% with high product purity.

The 1,2-HPON fluoresced at 458 nm, with a 38 nm difference between excitation and emission peaks, while the 2,3-HPON is not fluorescent. When bound to diphenyl boron, the 1,2-HPON diphenyl boron complex had strong emission at 466 nm with three different excitation peaks resulting in various intensities of the same emission. This pattern of multiple excitation peaks correlating to a single emission peak is consistent with previously studied oxadiazole diphenyl boron.[54] In the previous case HPOP was complexed with diphenyl boron resulting in a similar excitation patter but an emission of 443 nm. This shows a minute bathochromic shift of approximately 20 nm by extending the π system. In the case of the 1,2-HPON boron difluoride complex, again there were multiple excitation peaks for the emission at 436 nm, all with varying intensities of the

emission. Thus the effectiveness of color tuning of the 1,2-HPON ligand was minimal resulting in an emission shift of only 10-20 nm.

The 2,3-HPON ligand is not fluorescent on its own. When chelated with the diphenyl boron it exhibited multiple excitation peaks with a single excitation peak at varying intensities at 506 nm. When chelated with boron difluoride, it again showed multiple excitation peaks of varying intensities at 492 nm. Again this shows that the electron environment of the boron has little effect on the emission tuning of the complex.

Summary and Conclusions

Our research into new luminescent oxadiazole boron complexes has shown that the major contributing aspect of tuning these new emissive compounds is the isomeric substitution of the oxadiazole ligand and its resulting resonance. Through careful extension of the π system of the oxadiazole ligand we have shown this causes a minimal bathochromic shift of approximately 20nm on the overall fluorescence of the ligand as well as the boron complexes. The original benzoboroxole oxadiazole complexes did not form. This could be the result of many factors. The most likely causes are the oxadiazoles affinity for hydrogen bonding preventing the removal of water from the reaction before it reverses into the separate starting materials. It could also be caused by the oxygen atom in the heterocyclic ring on the benzoboroxole removing too much electron density from the boron combined with the inherent electron deficiency of the oxadiazole ring. However the use of more simplistic boron compounds has shown clear tetra-coordinated boron oxadiazole complexes with clear dative bond formation. The use of EWD and EDG on the boron compound also show minimal cytochromatic and bathochromatic shifts of approximately 10 nm respectively. These shifts were much smaller than anticipated. It

was assumed that the combination of π system augmentation and EDG would have a more significant effect on the fluorescence. The distinct change in fluorescence of the 2,3-HPON when complexed with either boron compound shows the most efficient tuning method lies in the substitution and resonance of the oxadiazoles extended conjugate system **Table1**. These complexes proved to rapidly decompose in the presence of water, even with the use of the hydrophobic diphenyl boron complex. This is most noticeable in the boron difluoride complex where the LCMS spectra shows the presence on only one fluoride atom due to decomposition from the minuscule amount of water in the solvent. The loss of two mass units indicates the formation of a BFOH oxadiazole complex with both the 1,2-HPON and 2,3 HPON ligands. Future research into this discovery will include other isomers of the HPON and further extension of the π system as well as the addition of more hydrophobic groups on the boron compounds to improve the complexes' stability in the presence of water.

Compound Name	**Excitation Wavelength (nm)**	**Emission Wavelength (nm)**
HPOP	387	458
BPh_2(POP)(THF)	257,304,338,406	443
1,2-HPON	396	458
BPh_2(1,2-PON)	326, 384, 425	468
BF_2(1,2-PON)	314, 341, 381, 397	436
BPh_2(2,3-PON)	326, 436	504
BF_2(2,3-PON)	343, 407	492

Table 1 The excitation and emission data of the oxadiazole complexes

Chapter 3

NMR Spectroscopy

All spectra were taken on a Varian INOVA 500 MHz NMR spectrophotometer maintained at 25 degrees Celsius operating at 500 MHz for 1H NMR and 126 MHz for 13C NMR. The deuterated solvent used for each respective spectrum is referenced to the appropriate literature peak shift. Refer to the appendix for all experimental spectra.

UV-Vis Spectroscopy

UV-vis spectra were all taken at less than $1.0x10^{-5}$ M using a JASCO V-670 spectrophotometer with a 1 nm band pass, using toluene as the solvent.

LC-MS Spectroscopy

All LC-MS spectra were taken on a Thermo Ultimate 3000 & Bruker micro OTOF-QIII using tetrahydrofuran as the solvent, with a concentration of 10 ppm.

Synthesis of Benzoboroxole

In a 500 mL round bottom flask at 0° C was added 2-formylphenylboronic acid (5.0183 g, 33.4709 mmol) and methanol (250 mL). Sodium borohydride (1.381 g, 35.1445 mmol) was slowly added to the solution over a period of approximately 5 minutes. The mixture was then stirred and removed from the ice bath allowing the flask to gradually warm to room temperature for a period of roughly 4 hours. With the formation of various salts, the solution became cloudy. This was then acidified by drop wise addition of HCl (3M, 5 mL) and extracted with ethyl acetate (3x20 mL). The

organic layer was then concentrated in vacuo to yield pure benzoboroxole (3.8285 g, 86.7% yield). Refer to the appendix for experimental data.

Synthesis of 6-Nitro-benzoboroxole

In a 50 mL round bottom flask at -40° C was added 25 ml of ≥90% fuming nitric acid. The benzoboroxole (5.291 g, 40.01 mmol) was added over a period of 10 min while stirring. A thick yellow/brown slurry was formed. The slurry was stirred at -40° C for 20 minutes. The slurry was added to 500 mL of ice water dropwise and stirred for 2 hours. A fine white precipitate formed. The product was recovered by vacuum filtration and washed (3 x 25 mL) with cold water. The resulting powder was allowed to air dry overnight yielding pure 6-nitro-benzoboroxole (6.7417 g, 93% yield)

Synthesis of 6-Amino-benzoboroxole

In a 250 mL round bottom flask 6-nitro-benzoboroxole (5.0132 g, 28.016 mmol), ammonium formate (8.83 g, 63.0599 mmol), palladium catalyst (1 g , 200mg Pd/C : 1 g 6-nitro-benzoboroxole) and anhydrous THF was stirred and allowed to reflux at 60° Celsius for 3 hours. The yellow solution was filtered to remove the residual palladium/carbon catalyst. The filtrate was concentrated in vacuo to yield reasonably pure 6-amino-benzoboroxole as a fine yellow powder that was used without further purification (3.3866 g, 81.2% yield).

Synthesis of 6-Dimethylamino-benzoboroxole

In a 50 mL round bottom flask 6-amino-benzoboroxole (270 mg, 1.812 mmol), potassium carbonate (1.25 g, 9.064 mmol), and acetone (25 mL) was stirred while iodomethane (0.33 mL, 5.438 mmol) was added dropwise. The reaction mixture was stirred for 30

minutes, then filtered to remover the potassium carbonate and washed with diethyl ether (2 x 10 mL). The filtrate was dried with magnesium sulfate, then concentrated in vacuo to produce pure 6-dimethylamino-benzoboroxole as an orange powder (300 mg, 93% yield).

Synthesis of Methyl 4-methoxy-2-naphthoate

In a 150 mL Erlenmeyer flask 1-hydroxy-2-naphthanoic acid (6.05 g, 32.15 mmol) and DMF (50 mL) was stirred until the solid completely dissolved. Potassium carbonate (16.57 g, 128.6 mmol) was added slowly to the solution as it stirred until the solution stopped evolving gas. Dropwise over approximately 5 minutes iodomethane (10 mL, 160.75 mmol) was added to the solution and allowed to stir over night. The solution was filtered to remove the remaining potassium carbonate, and the potassium carbonate was washed with DMF (3 X 10 mL). The filtrate was then extracted with diethyl ether and washed with cold water (5 X 20 mL), then dried over magnesium sulfate. The filtrate was then concentrated in vacuo to produce a pure methyl-4-methoxy-2-naphthoate as a viscous brown oil (5.94 g, 85% yield).

Synthesis of 4-methoxy-2-naphthohydrazide

In a 100 mL round bottom flask a mixture of methyl 4-methoxy-2-naphthoate (6.227 g, 28.796 mmol), hydrazine hydrate (6.4 mL, 55% N_2H_4), and ethanol (25 mL) was heated to 70° Celsius with a condenser overnight. The solution was concentrated in vacuo yielding reasonably pure, the primary impurity being water, 4-methoxy-2-naphthohydrazide as a brown powder that was used without further purification (7.598 g, yield almost quantitative, with some additional moisture in the compound).

Synthesis of N'-benzoyl-4-methoxy-2-naphthohydrazide

To a mixture of 4-methoxy-2-naphthohydrazide (7.598 g, 35.139 mmol) and pyridine (100 mL) in a 250 mL flask cooled to 0° Celsius, was added benzoyl chloride (7.5 mL) dropwise over approximately 20 minutes. The solution was stirred and kept cool for 2 hours, then allowed to stir at room temperature overnight. A creamy white precipitate was obtained and collected after the solution was added to 500 mL of ice/water. The precipitate was washed with water (3 x 25 mL), then allowed to air dry over 24 hours yielding pure N'-benzoyl-4-methoxy-2-naphthohydrazide as a white powder (10.022g, 89% yield).

Synthesis of 2-(1-methoxynaphthalen-2-yl)-5-phenyl-1,3,4-oxadiazole

In a 250 mL round bottom flask N'-benzoyl-4-methoxy-2-naphthohydrazide (10.15 g, 32.371 mmol) and phosphoryl chloride (100 mL) was refluxed for 24 hours. The resulting yellow solution was added to 500 mL of ice/water dropwise, producing a fine white precipitate. The precipitate was recrystallized from ethanol producing pure 2-(1-methoxynaphthalen-2-yl)-5-phenyl-1,3,4-oxadiazole as a fine white powder (6.74 g, 69% yield).

*Synthesis of 2-(5-phenyl-1,3,4-oxadiazol-2-yl)naphthalen-1-ol (**1,2-HPON**)*

In a 100 mL round bottom flask 2-(1-methoxynaphthalen-2-yl)-5-phenyl-1,3,4-oxadiazole (4.24 g, 14.024 mmol) was dissolved in 2,4,6-lutidiene (25 mL). Then lithium iodide (95.63 g, 42.073 mmol) was added to the solution over a period of 2 minutes. The solution was heated to reflux with a condenser column packed with Dryrite. Once at reflux the condenser was sealed with a cap to minimize water exposure from the air. The

reaction was allowed to reflux for 24 hours. The resulting yellow solution and black precipitate was acidified with hydrochloric acid (2M), yielding a fine grey precipitate. The precipitate was recovered via filtration and washed with water (3 X 20 mL) yielding pure 2-(5-phenyl-1,3,4-oxadiazol-2-yl)naphthalen-1-ol as a grey powder (3.881 g, 96% yield).

Synthesis of 2-(1-((diphenylboranyl)oxy)naphthalen-2-yl)-5-phenyl-1,3,4-oxadiazole

In a 100 mL round bottom flask 2-(5-phenyl-1,3,4-oxadiazol-2-yl)naphthalen-1-ol (228 mg, 1 mmol) was dissolved in anhydrous THF. The solution was cooled to 0° C. Then triphenyl boron: THF solution (0.25M, 4 mL) was added dropwise and stirred until the reaction reached room temperature. After 2 hours pure 2-(1-((diphenylboranyl)oxy)naphthalen-2-yl)-5-phenyl-1,3,4-oxadiazole was precipitated as a pale yellow solid and filtered (0.3026 g, 66.8% yield).

Synthesis of 2-(1-((difluoroboranyl)oxy)naphthalen-2-yl)-5-phenyl-1,3,4-oxadiazole

In a 100 mL round bottom flask 2-(5-phenyl-1,3,4-oxadiazol-2-yl)naphthalen-1-ol (200 mg, .6936 mmol) was dissolved in DCM and cooled to 0° Celsius. Then a boron trifluoride: methanol solution (14%, .08 mL) was added dropwise and stirred until room temperature was reached. A tan precipitate was formed and filtered off, yielding pure 2-(1-((difluoroboranyl)oxy)naphthalen-2-yl)-5-phenyl-1,3,4-oxadiazole as a fine tan powder (0.187 g, 75.7% yield).

Synthesis of Methyl 3-methoxy-2-naphthoate

In the same manner as the synthesis of Methyl 4-methoxy-2-naphthoate, the reaction of 2-hydroxy-3-naphthanoic acid (1.00 g, 5.343 mmol) and iodomethane (0.66 mL, 26.716

mmol) was concentrated in vacuo yielding Methyl 3-methoxy-2-naphthoate as a viscous brown oil (1.129 g, 97.8% yield). Refer to the appendix for experimental data.

Synthesis of 3-methoxy-2-naphthohydrazide

In the same manner as the synthesis of 4-methoxy-2-naphthohydrazide, the reaction of 3-methoxy-2-naphthohydrazide (3.86 g, 17.850 mmol) and hydrazine (4 mL, 79.92 mmol) was concentrated in vacuo yielding 3-methoxy-2-naphthohydrazide as a fine white powder (3.73 g, 96.7% yield). Refer to the appendix for experimental data.

Synthesis of N'-benzoyl-3-methoxy-2-naphthohydrazide

In the same manner as the synthesis of N'-benzoyl-4-methoxy-2-naphthohydrazide, the reaction of 3-methoxy-2-naphthohydrazide (1.681 g, 7.774 mmol) and benzoyl chloride (1.68 mL, 11.951 mmol) was washed with water yielding pure N'-benzoyl-3-methoxy-2-naphthohydrazide as a fine white powder (2.160 g, 87.2 % yield). Refer to the appendix for experimental data.

Synthesis of 2-(1-methoxynaphthalen-2-yl)-5-phenyl-1,3,4-oxadiazole

In the same manner as the synthesis of 2-(1-methoxynaphthalen-2-yl)-5-phenyl-1,3,4-oxadiazole, the reaction of Phosphoryl chloride (1.681 g, 7.774 mmol) and Phosphoryl chloride (1.68 mL, 11.951 mmol) was washed with water yielding pure 2-(1-methoxynaphthalen-2-yl)-5-phenyl-1,3,4-oxadiazole as a fine white powder (2.160 g, 87.2 % yield). Refer to the appendix for experimental data.

*Synthesis of Synthesis of 3-(5-phenyl-1,3,4-oxadiazol-2-yl)naphthalen-2-ol (**2,3HPON**)*

In the same manner as the synthesis of 1,2-HPON, 2-(1-methoxynaphthalen-2-yl)-5-phenyl-1,3,4-oxadiazole (0.5057 g, 1.672 mmol) and Lithium Iodide (0.6716 g, 5.018 mmol) was reacted for 24 hours yielding 2,3-HPON (0.2142 g, .7429 mmol) as a fine gray powder.

Synthesis of 3-(1-((diphenylboranyl)oxy)naphthalen-2-yl)-5-phenyl-1,3,4-oxadiazole

In the same manner of synthesis of 2-(1-((diphenylboranyl)oxy)naphthalen-2-yl)-5-phenyl-1,3,4-oxadiazole, 2,3-HPON (.2880 g, 1.0 mmol) was reacted with triphenyl borane (0.25M, 4 mL) was reacted at RT yielding 2-(1-((diphenylboranyl)oxy)naphthalen-2-yl)-5-phenyl-1,3,4-oxadiazole (0.3026 g, 66.8 % yield) as a fine yellow powder.

Synthesis of 3-(1-((difluoroboranyl)oxy)naphthalen-2-yl)-5-phenyl-1,3,4-oxadiazole

In the same manner of synthesis as 2-(1-((difluoroboranyl)oxy)naphthalen-2-yl)-5-phenyl-1,3,4-oxadiazole, 2,3-HPON (0.255 g, 0.8844 mmol) and trifluoroborane methanol solution (14%, 0.113 mL) was added dropwise and reacted in methanol for 2 hours, yielding 3-(1-((difluoroboranyl)oxy)naphthalen-2-yl)-5-phenyl-1,3,4-oxadiazole (0.125 g, 42.1 % yield)

Bibliography

(1) Weeks, M. E. *In Discovery of the Elements*; Kessinger Publishing Reprints, **1933**; p. 380.

(2) Laubengayer, A.; Hurd, D.; Newkirk, A.; Hoard, J. *Journal of the American Chemical Society* **1943**, 65, 1924-1931.

(3) Argust, P. *Biological Trace Element Research* **1998**, 66, 131-143.

(4) *The Economics of Boron*; 11th ed.; Roskill Information Services Limited, **2006**.

(5) Atkins, P.; Overton, T.; Rourke, J.; Weller, M.; Armstrong, F. Shriver & Atkins, *Inorganic Chemistry*; 4th ed.; Oxford University Press: New York, **2006**.

(6) Krishnamurthy, S.; Brown, H. *Aldrichimica Acta* **1979**, 12, 1-12.

(7) Brown, H.; Krishnamurthy, S. *Journal of the American Chemical Society* **1974**, 95, 1669.

(8) Brown, H.; Ramachandran, P. *Journal of Organometallic Chemistry* **1995**, 500, 1-19.

(9) Soundararajan, R.; Matteson, D. *Journal of Organic Chemistry* **1990**, 55, 2274-2275.

(10) Luche, J.; Gemal, A. *Journal of the American Chemical Society* **1981**, 103, 5454-5459

(11) Yin, L.; Liebscher, J. *Chemical Reviews* **2007**, 107, 133-173.

(12) X. Hui, S.J. Baker, R.C Wester, S. Barbadillo, A. K. Cashmore, V. Sanders, K. M. Hold, T. Akama, Y.-K. Zhang, J. J. Plattner, H. I. Maibach, *J. Pharm. Sci.* **2007**, 96, 2622.

(13) a) S.J. Baker, C. Z. Ding, T. Akama, Y. K. Zhang, V. Hernandez, Y. Xia, *Future Med. Chem.* **2009**, 1, 1275;

b) Anacor Pharmacueticals, US 234981(A1)**2006**

(14) Y.-K. Zhang, J. J. Plattner, Y. R. Freund, E. E. Easom, Y. Zhou, L. Ye, H. Wange, H. Cui. *Bioorg. Med Chem. Lett.* **2012**, 22,1299.

(15) R.T. Jacobs, J. J. Plattner, B. Nare, S. A. Wring, D. Chen, Y. Freund, E. G. Gaukel, M. D. Orr, J. B. Perales, M. Jenks, R. A. Noe, J. M. Sligar, Y. –K. Zhang, C. J. Bacchi, N. Yarlett, R. Don, *Future Med. Chem.* **2011**, 9, 199.

(16) Barth, R. F.; Coderre, J. A.; Vicente, M. G. H.; Blue, T. E. *Clinical cancer research* **2005**, 11, 39874002.

(17) Hattori, S.; Ohkubo, K.; Urano, Y.; Sunahara, H.; Nagano, T.; Wada, Y.; Tkachenko, N. V.; Lemmetyinen, H.; Fukuzumi, S. *The Journal of Physical Chemistry B* **2005**, 109, 15368-15375.

(18) Imahori, H.; Norieda, H.; Yamada, H.; Nishimura, Y.; Yamazaki, I.; Sakata, Y.; Fukuzumi, S. *Journal of the American Chemical Society* **2001**, 123, 100-110.

(19) Kollmannsberger, M.; Rurack, K.; Resch-Genger, U.; Daub, J. *The Journal of Physical Chemistry A* **1998**, 102, 10211-10220.

(20) Rao, Y.; Amarne, H.; Zhao, S.; McCormick, T. M.; MarOć, S.; Sun, Y.; Wang, R.; Wang, S. *Journal of the American Chemical Society* **2008**, 130, 12898-12900.

(21) Boyer, J. H.; Haag, A. M.; Sathyamoorthi, G.; Soong, M.; Thangaraj, K.; Pavlopoulos, T. G. *Heteroatom Chemistry* **1993**, 4, 39-49.

(22) Entwistle, C. D.; Marder, T. B. *Angewandte Chemie International Edition* **2002**, 41, 2927-2931.

(23) Branger, C.; Lequan, M.; Lequan, R.; Large, M.; Kajzar, F. *Chemical Physics Letters* **1997**, 272, 265-270.

(24) Zeng, L.; Miller, E. W.; Pralle, A.; Isacoff, E. Y.; Chang, C. J. *Journal of the American Chemical Society* **2006**, 128, 10-11.

(25) Killoran, J.; Allen, L.; Gallagher, J. F.; Gallagher, W. M.; OShea, D. F. *Chem. Commun.* **2002**, 18621863.

(26) Kubo, Y.; Yamamoto, M.; Ikeda, M.; Takeuchi, M.; Shinkai, S.; Yamaguchi, S.; Tamao, K. *Angewandte Chemie International Edition* **2003**, 42, 2036-2040.

(27) Burghart, A.; Thoresen, L. H.; Chen, J.; Burgess, K.; Bergström, F.; Johansson, L. B. *Chem. Commun.* **2000**, 2203-2204.

(28) Murata, N.; Haruyama, J.; Reppert, J.; Rao, A. M.; Koretsune, T.; Saito, S.; Matsudaira, M.; Yagi, Y. *Phys. Rev. Lett.* **2008**, 101.

(29) Gajewski, W.; Achatz, P.; Williams, O. A.; Haenen, K.; Bustarret, E.; Stutzmann, M.; Garrido, J. *A. Phys. Rev. B* **2009**, 79.

(30) Yamaguchi, S.; Akiyama, S.; Kohei, T. *Journal of the American Chemical Society* **2001**, 123, 1137211375.

(31) Cui, Y.; Li, F.; Lu, Z.; Wang, S. *Dalton Trans*. **2007**, 2634.

(32) Sun, Y.; Wang, S. *Inorganic Chemistry* **2009**, 48, 3755-3767.

(33) Yamaguchi, S.; Shirasaka, T.; Akiyama, S.; Tamao, K. *Journal of the American Chemical Society* **2002**, 124, 8816-8817.

(34) Zhao, S.; McCormick, T.; Wang, S. Inorganic Chemistry 2007, 46, 10965-10967.

(35) John A. Joule; Keith Mills, *Heterocyclic Chemistry*, **2013**, 842.

(36) P. Sengupta, M. Mal, S. Mandal, J. Singh, T. K. Maity, *Iranian Journal of Pharmacology and Therapeutics*, vol. 7, no. 2, pp. 165-167, **2008**.

(37) A. A. Kadi, N. R. El-Brollosy, O. A. Al-Deeb, E. E. Habib, T. M. Ibrahim, A. A. El-Emam, *European Journal of Medicinal Chemistry*, vol. 42, no. 2, pp. 235-242, **2007**.

(38) N. Bhardwaj, S. K. Saraf, P. Sharma, P. Kumar, *E-Journal of Chemistry*, vol. 6, no. 4, pp. 1133-1138, **2009**.

(39) M. A. Bakht, M. S. Yar, S. G. Abdel-Hamid, S. I. Al Qasoumi, A. Samad, *European Journal of Medicinal Chemistry*, vol. 45, no. 12, pp. 5862-5869, **2010**.

(40) M. J. Ahsan, J. G. Samy, H. Khalilullah et al., *Bioorganic and Medicinal Chemistry Letters*, vol. 21, no. 24, pp. 7246-7250, **2011**.

(41) M. J. Ahsan, J. Sharma, S. Bhatia, P. K. Goyal, K. Shankhala, M. Didel, *Letters in Drug Design and Discovery*, vol. 11, no. 4, pp. 413-419, **2013**.

(42) G. C. Ramaprasad, B. Kalluraya, B. Sunil Kumar, S. Mallya, *Medicinal Chemistry Research*, vol. 22, no. 11, pp. 5381-5389, **2013**.

(43) Suman Bala, Sunil Kamboj, Anu Kajal, Vipin Saini, Deo Nanadan Prasad, *BioMed Research International*, vol. **2014**

(44) T. Akhtar, S. Hameed, N. A. Al-Masoudi, R. Loddo, P. L. Colla, *Acta Pharmaceutica*, vol. 58, no. 2, pp. 135-149, **2008**.

(45) M. Khan, T. Akhtar, N. A. Al-Masoudi, H. Stoeckli-Evans, and S. Hameed, *Medicinal Chemistry*, vol. 8, no. 6, pp. 1190-1197, **2012**.

(46) Salahuddin, M. Shaharyar, A. Majumdar, M. J. Ahsan, *Arabian Journal of Chemistry*, **2013**.

(47) M. J. Ahsan, J. G. Samy, C. B. Jain, K. R. Dutt, H. Khalilullah, and M. S. Nomani, *Bioorganic and Medicinal Chemistry Letters*, vol. 22, no. 2, pp. 969-972, **2012**.

(48) M. J. Ahsan, R. V. P. Singh, M. Singh et al*., Medicinal Chemistry*, vol. 33, no. 3, pp. 294-297, **2013**.

(49) Ahsan, Mohamed Jawed, et al. *BioMed Research International*, **2014**

(50) Wang, J. F., Jabbour, G. E., Mash, E. A., Anderson, J., Zhang, Y., Lee, P. A., Armstrong, N. R., Peyghambarian, N. and Kippelen, B. *Adv. Mater.* **1999**, 11: 1266–1269.

(51) Lianqing Chen, Han You, Chuluo Yang, Dongge Ma, Jingui Qin. *Chem. Commun*., **2007**, 1352–1354

(52) Jiun-Haw Lee a, Meng-Hsiu Wu, Chun-Chieh Chao, Hung-Lin Chen, Man-Kit Leung. *Chemical Physics Letters* 416. **2005**. 234–237

(53) Janghouri, Mohammad; Mohajerani, Ezeddin; Amini, Mostafa M, Najafi, Ezzatollah; Hosseini, Hadi. *Journal of Electronic Materials*, 42,10, **2013**. 2915-2925.

(54) Ruipig Deng, Leijiao Li, Mingxing Song, Shuna Zhao, Liang Zhao, Shuan Yoa. *The Royal Society of Chemistry 20*, **2016**. 1-11

(55) Shivashankar, Sunitha M., Vishnumurthy K. Anantapadmanabha, Airody Vasudeva Adhikari. *Polymer Engineering and Science* 53.6 **2013**

(56) G.D.L. Torre, P. Vazquez, F. Agullo-Lopez, and T. Torres, *Chem. Rev.*, 104, 3723 **2004**.

(57) D. Udayakumar and A.V. Adhikari, *Synth. Met.*, 156. 1168. **2006**

(58) Tang, C.; VanSlyke, S. *Applied Physics Letters* **1987**, 51, 913-915.

(59) Kulkarni, A. P.; Tonzola, C. J.; Babel, A.; Jenekhe, S. *A. Chemistry of Materials* **2004**, 16, 45564573.

(60) Hughes, G.; Bryce, M. R. *J. Mater. Chem.* **2005**, 15, 94.

(61) Boer, W. D. *Active Matrix Liquid Crystal Displays*; Newnes: Oxford, **2005**

(62) *Physical Properties of Liquid Crystals*: Nematics; Dunmur, D.; Fukuda, A.; Luckhurst, G., Eds.; Inspec/Iee: London, **2001**.

(62) www.nakan-tech.cp.jp <http://www.nakan-techno.co.jp/en/technology/glossary.html> 2 March 2016

(63) Kafafi, Z. *Organic Electroluminescence*; CRC Press, Taylor & Francis Group: Boca Raton, **2005**.

(64) Kalinowski, J. *Organic Light-Emitting Diodes: Principles, Characteristics, and Processes*; Marcel Dekker: New York, **2005**.

(65) *Organic Light-Emitting Materials and Devices*; Li, Z.; Meng, H., Eds.; CRC Press, Taylor & Francis Group: Boca Raton, **2007**.

(66) Wakamiya, A.; Mori, K.; Yamaguchi, S. Angew. *Chem. Int. Ed*. **2007**, 46, 4273-4276.

(66) Craig Freudenrich, Ph.D. "How OLEDs Work" 24 March 2005.

HowStuffWorks.com. <http://electronics.howstuffworks.com/oled.htm> 2 March 2016

(67) Jia, W.; Song, D.; Wang, S. The Journal of Organic Chemistry 2003, 68, 701-705.

(68) Cui, Y.; Wang, S. *The Journal of Organic Chemistry* **2006**, 71, 6485-6496.

(69) Qin, Y.; Kiburu, I.; Shah, S.; Jakle, F. *Macromolecules* **2006**, 39, 9041-9048.

(70) Qin, Y.; Kiburu, I.; Shah, S.; Jakle, F. *Organic Letters* **2006**, 8, 5227-5230.

(71) Liu, S.; Wu, Q.; Schmider, H. L.; Aziz, H.; Hu, N.; Popovic, Z.; Wang, S. *Journal of the American Chemical Society* **2000**, 122, 3671-3678.

(72) Liu, Q.; Mudadu, M. S.; Thummel, R.; Tao, Y.; Wang, S. Advanced Functional Materials 2005, 15, 143-154.

(73) Chen, H.; Chi, Y.; Liu, C.; Yu, J.; Cheng, Y.; Chen, K.; Chou, P.; Peng, S.; Lee, G.; Carty, A.; Yeh, S.; Chen, C. *Advanced Functional Materials* **2005**, 15, 567-574.

(74) Cotton, F.; Wilkinson, G. Advanced Inorganic Chemistry; 5th ed.; John Wiley and Sons Inc: New York, **1998**.

(75) Muetterties, E. *The Chemistry of Boron and Its Compounds*; John Wiley and Sons Inc: New York, **1967**.

(76) Hirao, H.; Fujimoto, H. *The Journal of Physical Chemistry A* **2000**, 104, 6649-6655.

(77) Kotz, J.; Treichel Jr., P. Chemistry and Chemical Reactivity; 4th ed.; Saunders College Publishing: Orlando, **1996**.

(78) Wakamiya, A.; Taniguchi, T.; Yamaguchi, S. Angew. *Chem. Int. Ed*. **2006**, 45, 3170-3173.

(79) Park, N. G.; Lee, J.; Park, Y. H.; Kim, Y. S. Synthetic Metals 2004, 145, 279-283.

(80) Wang, S. *Coordination Chemistry Reviews* **2001**, 215, 79-98.

(81) Wu, Q.; Esteghamatian, M.; Hu, N.; Popovic, Z.; Enright, G.; Tao, Y.; D'Iorio, M.; Wang, S. *Chem. Mater.* **2000**, 12, 79-83.

(82) Anderson, S.; Weaver, M. S.; Hudson, A. *J. Synthetic Metals* **2000**, 111, 459-463.

(83) Nagata, Y.; Chujo, Y. *Macromolecules* **2008**, 41, 3488-3492.

(84) Ugolotti, J.; Hellstrom, S.; Britovsek, G. J. P.; Jones, T. S.; Hunt, P.; White, A. J. P. *Dalton Trans*. **2007**, 1425.

(85) Kappaun, S.; Rentenberger, S.; Pogantsch, A.; Zojer, E.; Mereiter, K.; Trimmel, G.; Saf, R.; Möller, K. C.; Stelzer, F.; Slugovc, C. *Chem. Mater.* **2006**, 18, 3539-3547.

(86) Cui, Y.; Liu, Q.; Bai, D.; Jia, W.; Tao, Y.; Wang, S. *Inorganic Chemistry* **2005**, 44, 601-609

(87) Loudet, A.; Burgess, K. *Chemical Reviews* **2007**, 107, 4891-4932.

(88) Yang, G.; Su, T.; Su, Z.; Zhang, H.; Wang, Y. *J. Phys. Chem. A* **2007**, 111, 2739-2744.

(89) Zhang, H.; Huo, C.; Ye, K.; Zhang, P.; Tian, W.; Wang, Y. *Inorganic Chemistry* **2006**, 45, 2788-2794.

(90) Liddle, B. J.; Silva, R. M.; Morin, T. J.; Macedo, F. P.; Shukla, R.; Lindeman, S. V.; Gardinier, J. R. *The Journal of Organic Chemistry* **2007**, 72, 5637-5646.

(91) Cheng, C.; Yu, W.; Chou, P.; Peng, S.; Lee, G.; Wu, P.; Song, Y.; Chi, Y. *Chem. Commun.* **2003**, 2628.

(92) Liu, Q.; Mudadu, M. S.; Schmider, H.; Thummel, R.; Tao, Y.; Wang, S. *Organometallics* **2002**, 21, 4743-4749.

(93) Snyder, H.; Reedy, A.; Lennarz, W. *Journal of the American Chemical Society* **1958**, 80, 835-838.

(94) Haynes, R.; Snyder, H. *Journal of Organic Chemistry 1964*, 29, 3229-3233.

(95) Cummings, W.; Cox, C.; Snyder, H. *Journal of Organic Chemistry 1969*, 34, 1669-1674.

(96) Gunasekera, D. S.; Gerold, D. J.; Aalderks, N. S.; Chandra, J. S.; Maanu, C. A.; Kiprof, P.; Zhdankin, V. V.; Reddy, M. V. R. *Tetrahedron* **2007**, 63, 9401-9405.

(97) Brown, H.; Bhat, N.; Somayaji, V. *Organometallics* **1983**, 2, 1311-1316.

(98) Robin, B.; Buell, G.; Kiprof, P.; Nemykin, V. *Acta Crystallographica Section E E64*, o314-o315.

Appendix

All supporting experimental spectra and data are presented there within. Data is presented as per section of experiment; refer to the table of contents for pagination of material provided.

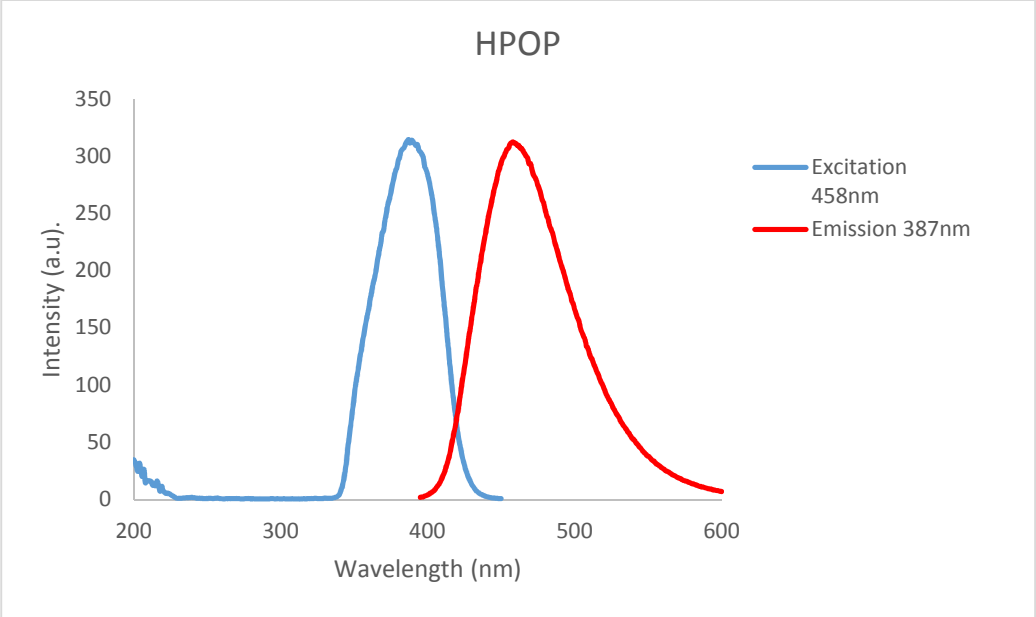

FIG 12 Excitation and emission data for HPOP

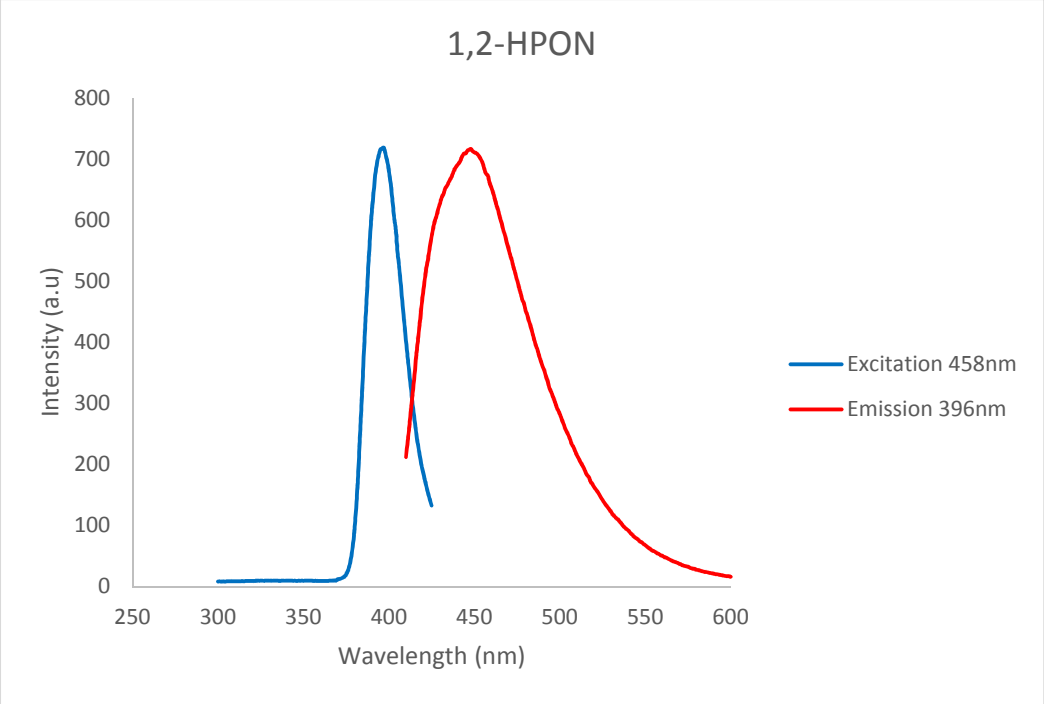

FIG 13 Excitation and emission data for 1,2-HPON

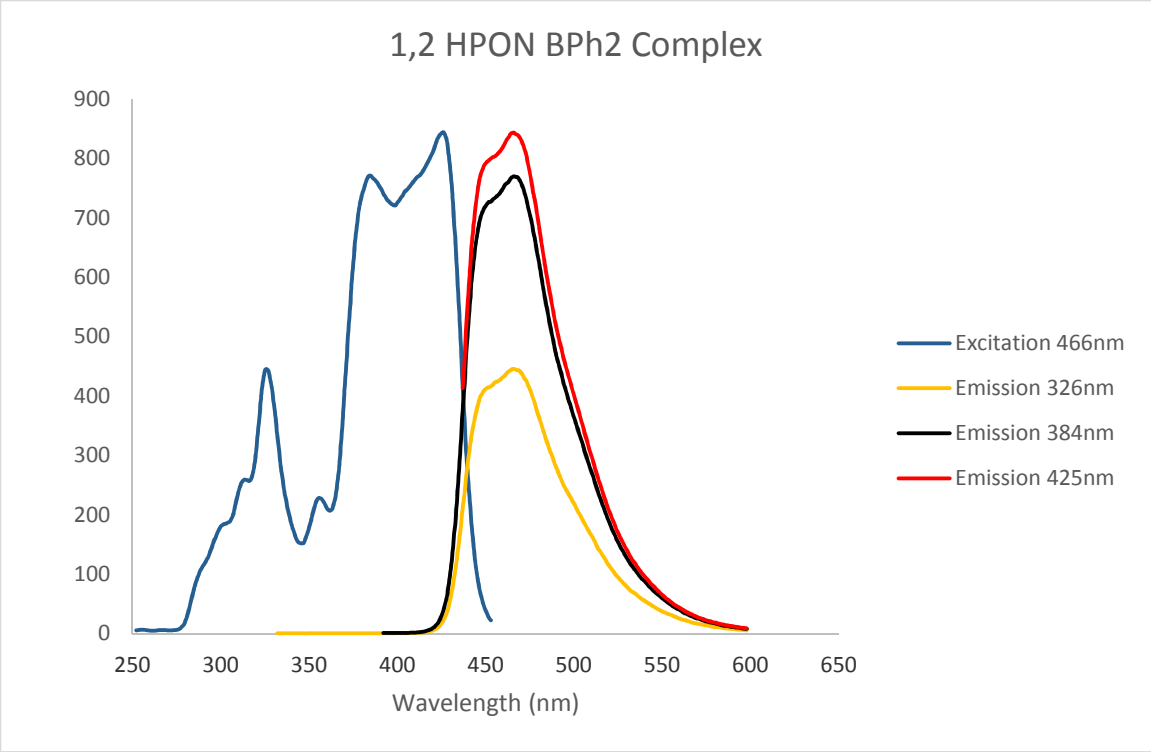

FIG 14 Excitation and emission data for BPh_2(1,2-PON)

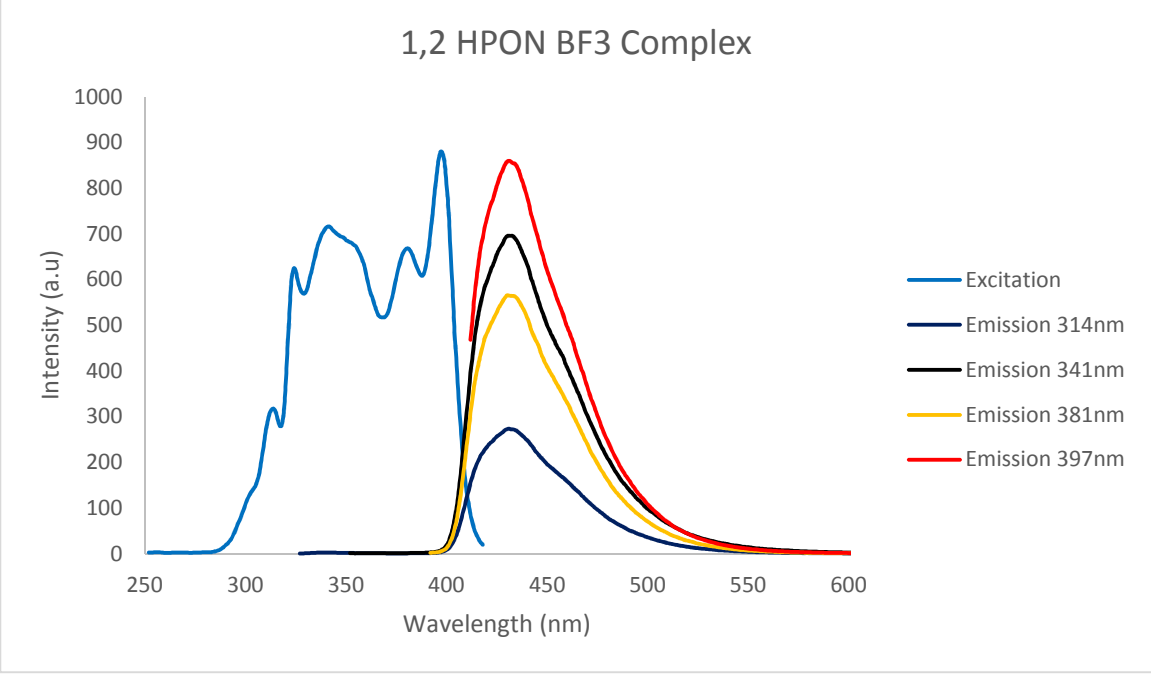

FIG 15 Excitation and emission data for BF_2(1,2-PON)

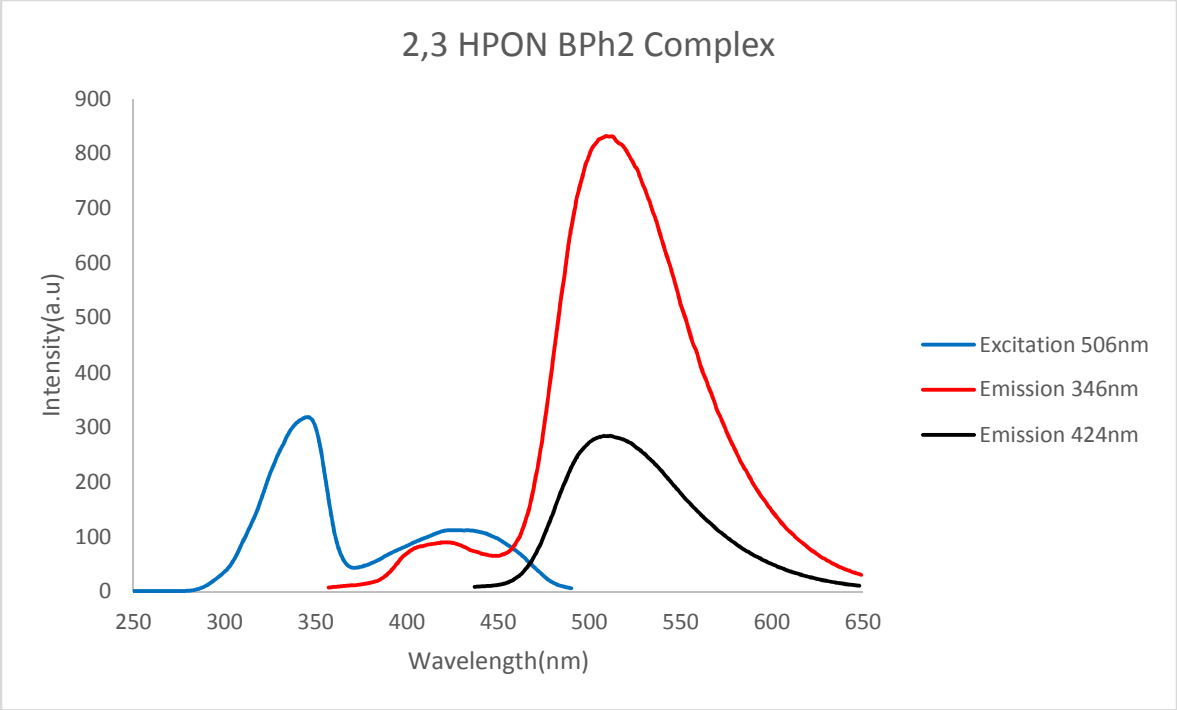

FIG 16 Excitation and emission data for BPh_2(2,3-PON)

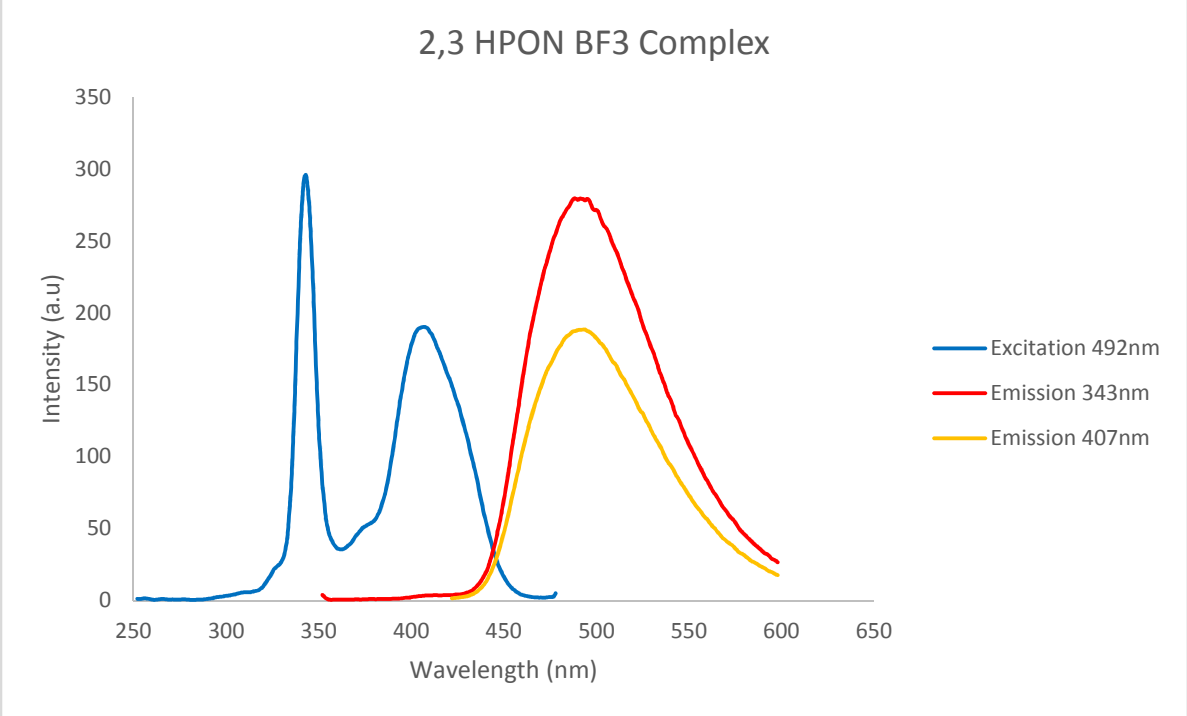

FIG 17 Excitation and emission data for BF_2(2,3-PON)

NMR Spectroscopy

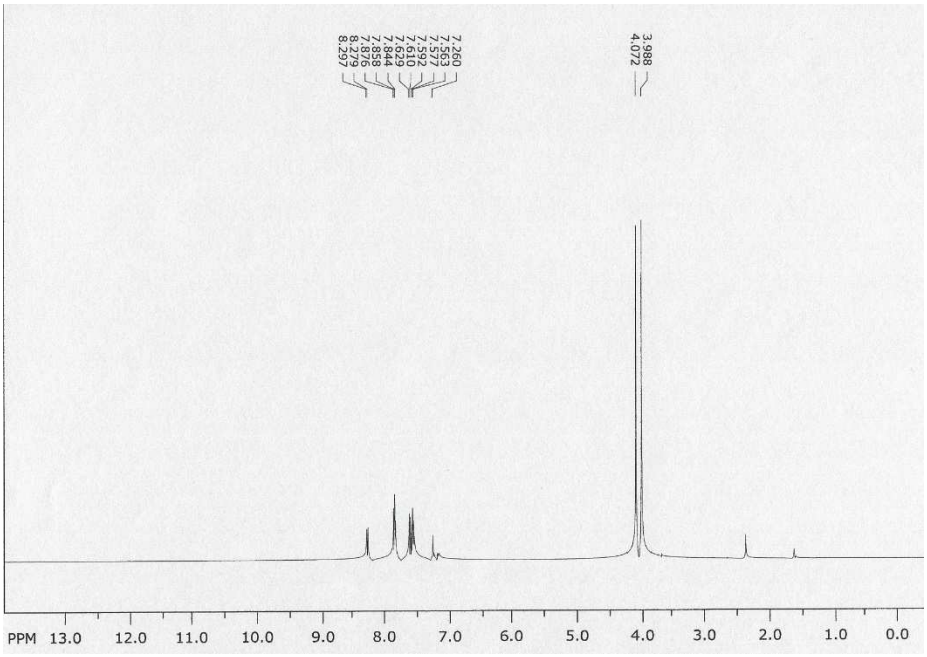

FIG 18 [1]HNMR Methyl 4-Methoxy-2-Naphthoate (500 MHz, $CDCl_3$) δ 8.297, 8.279, 7.876, 7.858, 7.844, 7.629, 7.610, 7.592, 7.577, 7.563, 4.072, 3.988

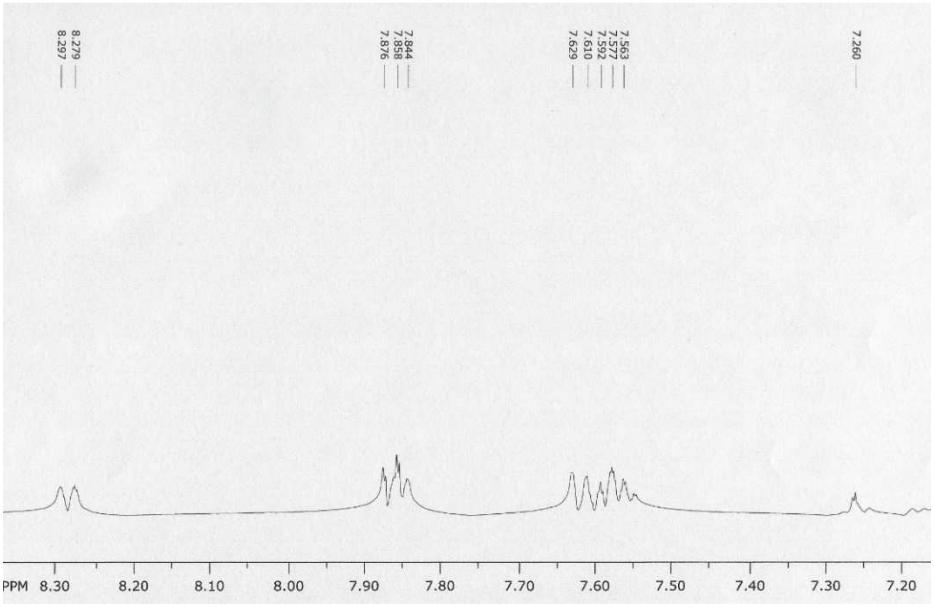

FIG 19 [1]HNMR Methyl 4-Methoxy-2-Naphthoate (500 MHz, $CDCl_3$) δ 8.297, 8.279, 7.876, 7.858, 7.844, 7.629, 7.610, 7.592, 7.577, 7.563, 4.072, 3.988

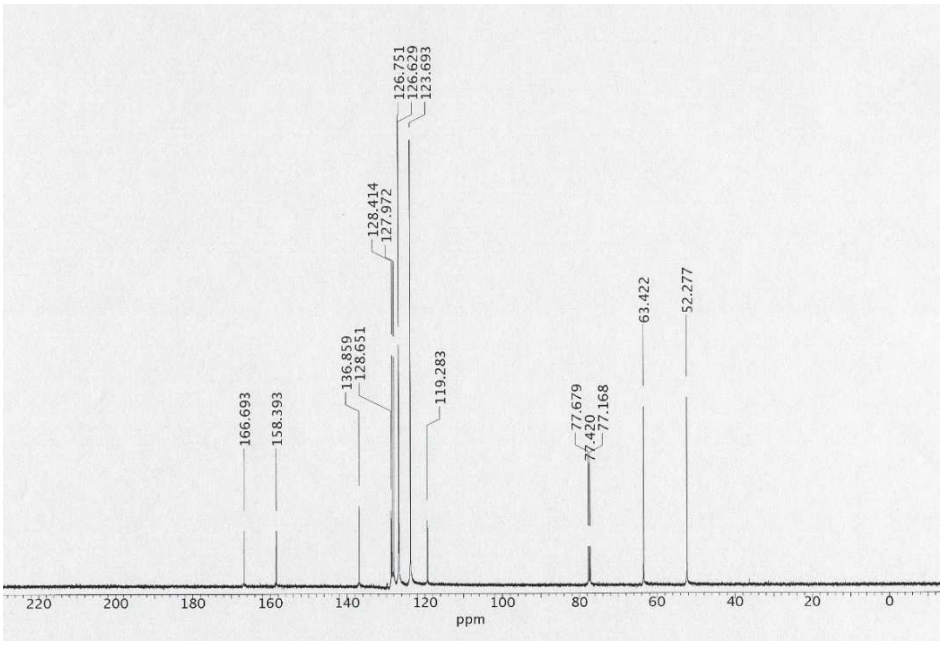

FIG 20 ^{13}CNMR Methyl 4-Methoxy-2-Naphthoate (500 MHz, $CDCl_3$) δ 166.693, 158.393, 136.859, 128.651, 128.414, 127.972, 126.751, 126.629, 123.693, 119.283, 63.422, 52.27

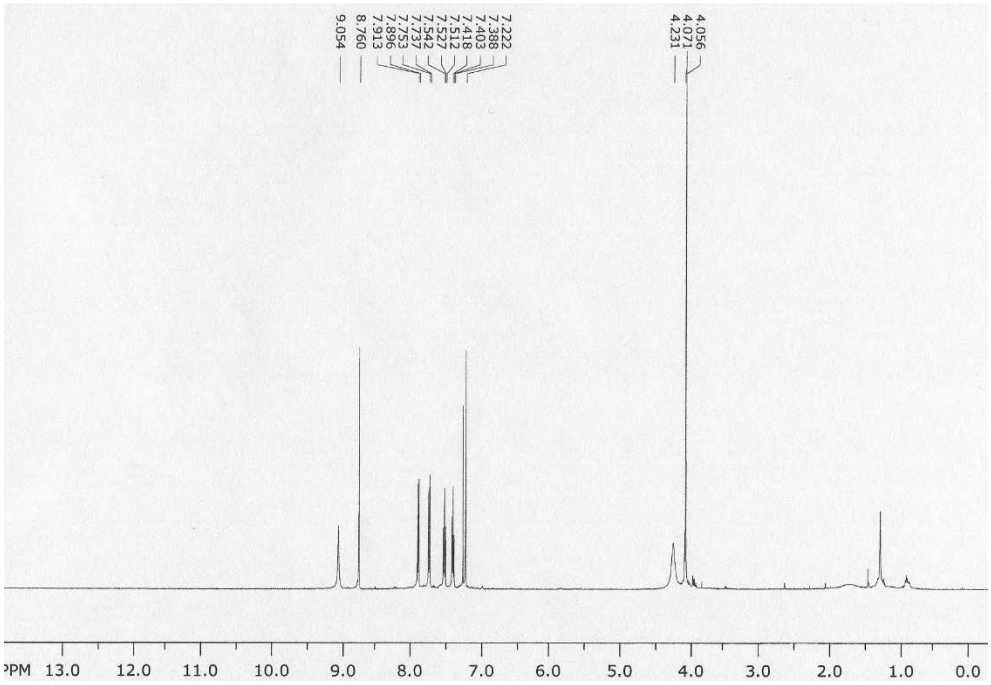

FIG 21 ^{1}HNMR 4-Methoxy-2-Naphthohydrazide (500 MHz, $CDCl_3$) δ 9.054, 8.760, 7.913, 7.869, 7.753, 7.737, 7.542, 7.527, 7.512, 7.418, 7.403, 7.388, 7.222, 4.231, 4.071, 4.056

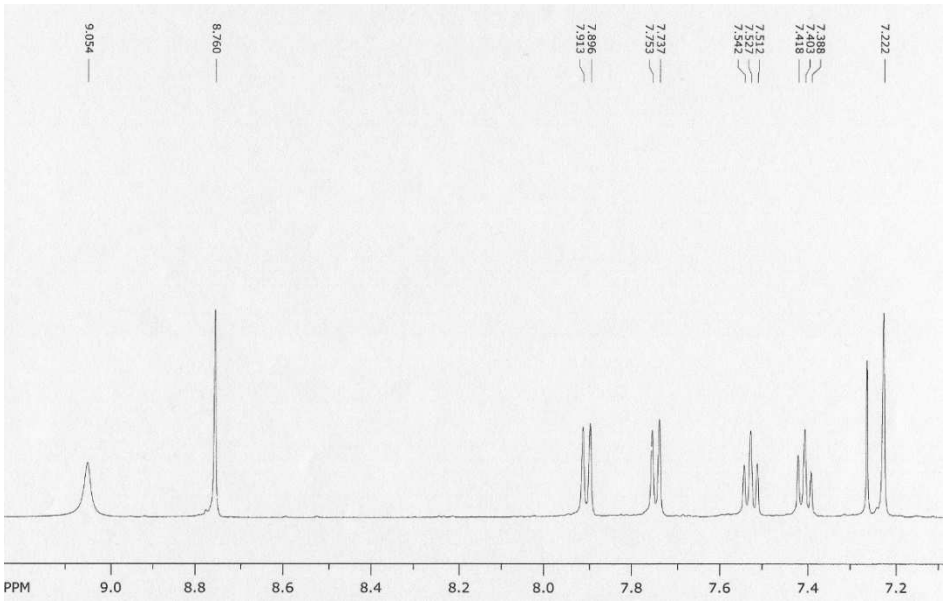

FIG 22 [1]HNMR 4-Methoxy-2-Naphthohydrazide (500 MHz, $CDCl_3$) δ 9.054, 8.760, 7.913, 7.869, 7.753, 7.737, 7.542, 7.527, 7.512, 7.418, 7.403, 7.388, 7.222, 4.231, 4.071, 4.056

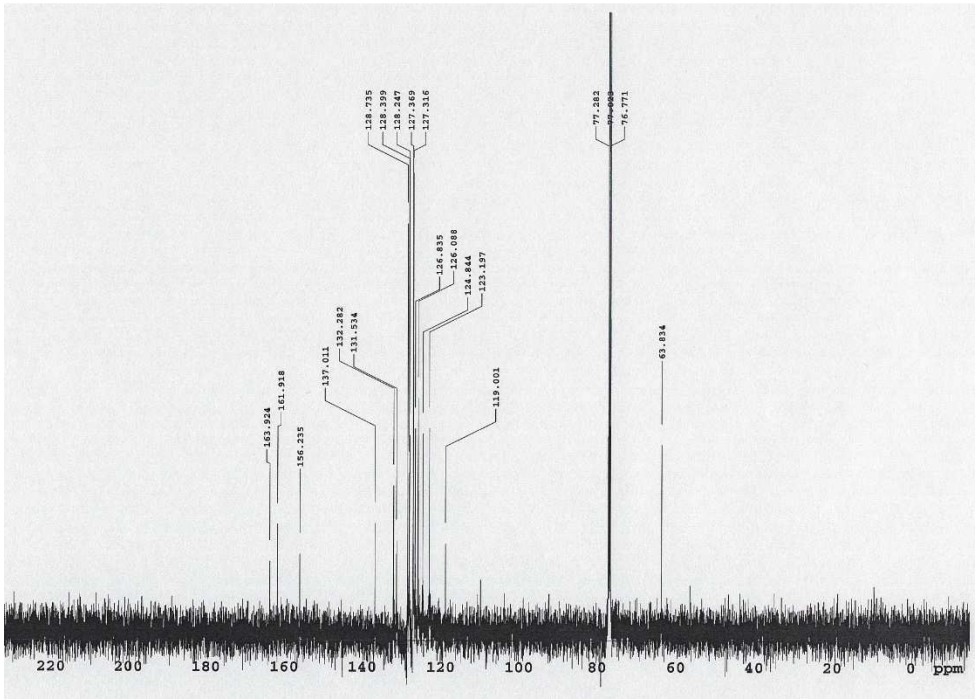

FIG 23 [13]CNMR 4-Methoxy-2-Naphthohydrazide (500 MHz, $CDCl_3$) δ 163.924, 161.918, 156.235, 137.011, 132.282, 131.534, 128.735, 128.399, 128.247, 127.369, 127.316, 126.835, 126.088, 124.844, 123.197, 119.001, 63.834

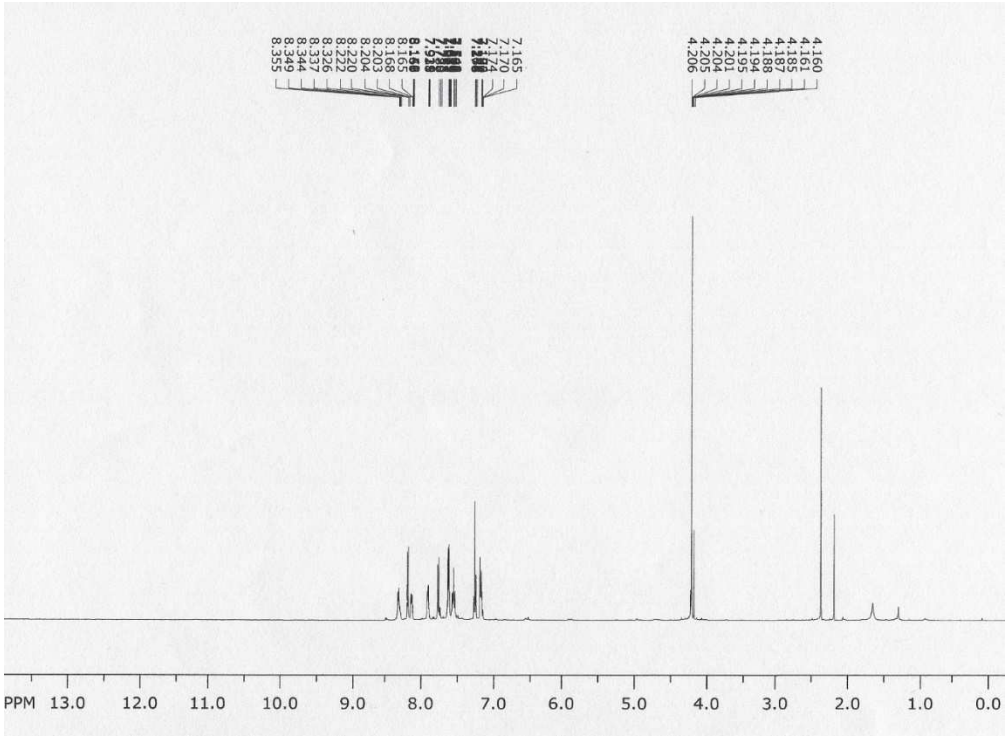

FIG 24 ^{1}HNMR N'-benzoyl-4-methoxy-2-naphthohydrazide (500 MHz, $CDCl_3$) δ 8.355, 8.349, 8.344, 8.337, 8.326, 8.222, 8.220, 8.204, 8.203, 8.168, 8.165, 8.155, 8.151, 8.149, 8.142, 7.93, 7.788, 7.770, 7.753, 7.653, 7.651, 7.645, 7.639, 7.633, 7.627, 7.625, 7.619, 7.581, 7.578, 7.562, 7.548, 7.286, 7.268, 7.190, 7.174, 7.170, 7.165, 4.206, 4.205, 4.204, 4.201, 4.195, 4.194, 4.188, 4.187, 4.185, 4.161, 4.160

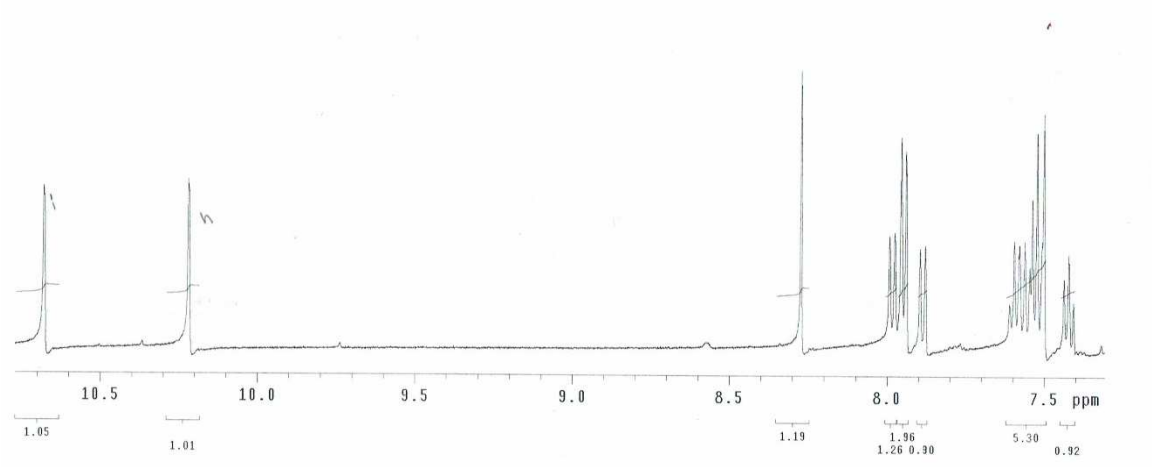

FIG 25 [1]HNMR N'-benzoyl-4-methoxy-2-naphthohydrazide (500 MHz, $CDCl_3$) δ 8.355, 8.349, 8.344, 8.337, 8.326, 8.222, 8.220, 8.204, 8.203, 8.168, 8.165, 8.155, 8.151, 8.149, 8.142, 7.93, 7.788, 7.770, 7.753, 7.653, 7.651, 7.645, 7.639, 7.633, 7.627, 7.625, 7.619, 7.581, 7.578, 7.562, 7.548, 7.286, 7.268, 7.190, 7.174, 7.170, 7.165, 4.206, 4.205, 4.204, 4.201, 4.195, 4.194, 4.188, 4.187, 4.185, 4.161, 4.160

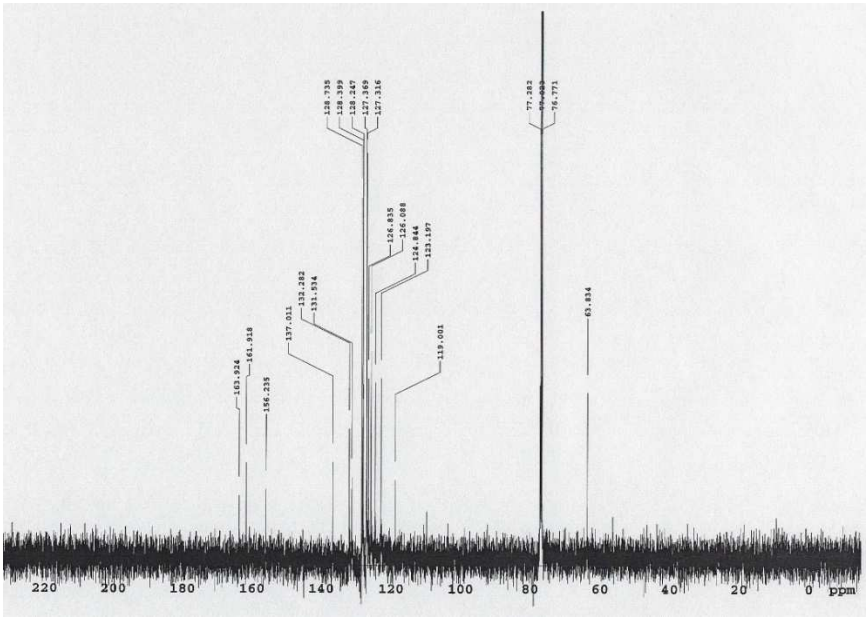

FIG 26 [13]CNMR N'-benzoyl-4-methoxy-2-naphthohydrazide (500 MHz, $CDCl_3$) δ 163.924, 161.918, 156.235, 137.011, 132.282, 131.534, 128.735, 128.399, 128.247, 127.369, 127.316, 126.835, 126.088, 124.844, 123.197, 119.001, 63.834

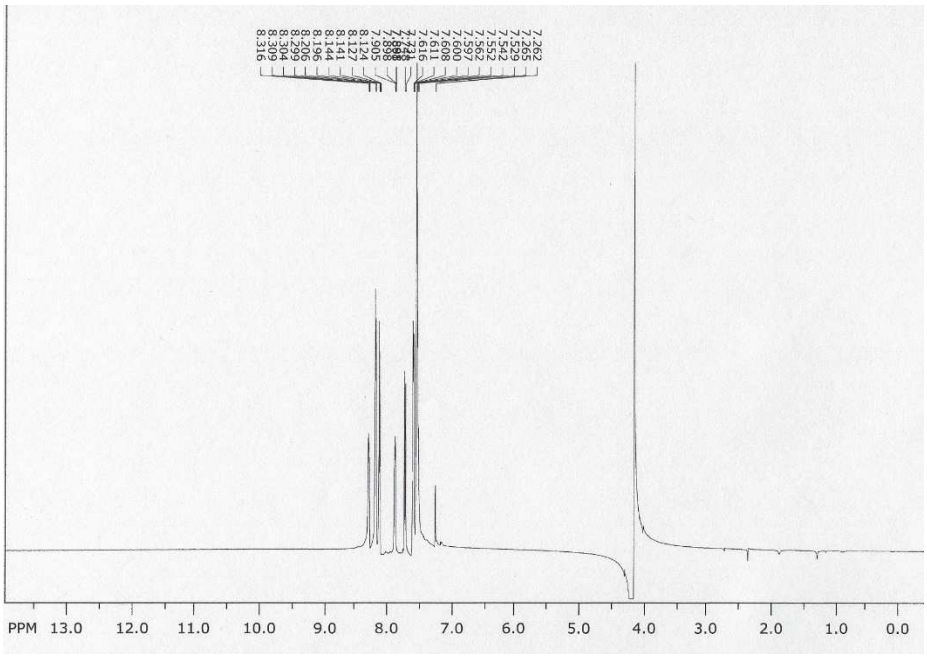

FIG 27 ^{1}HNMR 2-(1-methoxynaphthalen-2-yl)-5-phenyl-1,3,4-oxadiazole (500 MHz, $CDCl_3$) δ 8.316, 8.309, 8.304, 8.299, 8.206, 8.196, 8.144. 8.141, 8.127, 8.124, 7.905, 7.898, 7.895, 7.891, 7.888, 7.748, 7.731, 7.616, 7.611, 7.608, 7.600, 7.597, 7.562, 7.552. 7.542, 7.529, 4.328

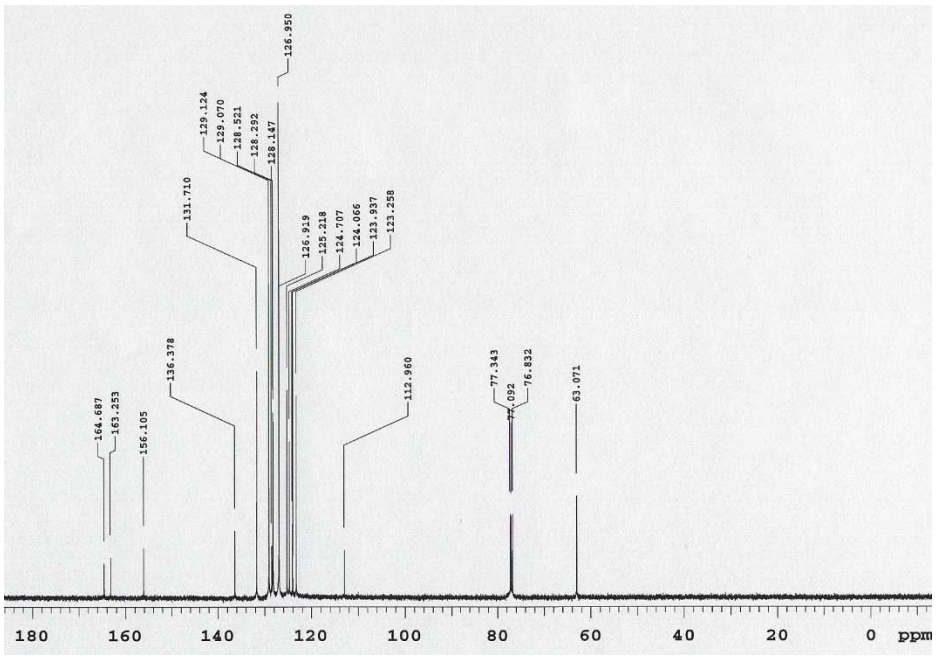

FIG 28 ^{13}CNMR 2-(1-methoxynaphthalen-2-yl)-5-phenyl-1,3,4-oxadiazole (500 MHz, $CDCl_3$) δ 164.687, 163.253, 156.105, 136.378, 131.710, 129.124, 129.070, 128.292, 128.147, 126.950, 126.919, 125.218, 124.707, 124.066, 123.937, 123.258, 112.960, 63.071

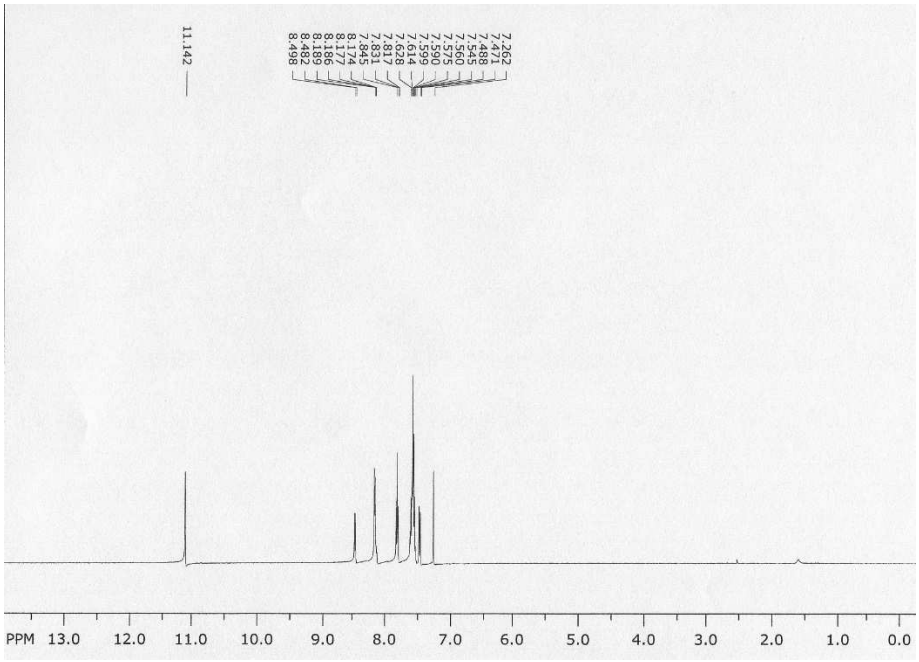

FIG 29 [1]HNMR 1,2-HPON (500 MHz, CDCl3) δ 11.142, 8.498, 8.482, 8.189, 8.177, 8.174, 7.845, 7.831, 7.817, 7.628, 7.628, 7.614, 7.599, 7.590, 7.575, 7.560, 7.545, 7.488, 7.471

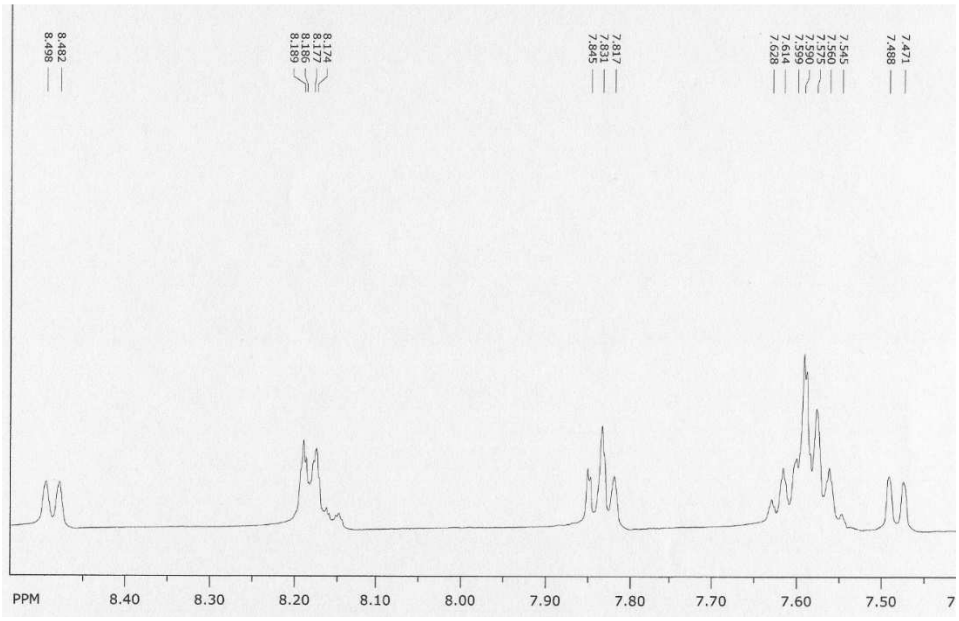

FIG 30 [1]HNMR 1,2-HPON (500 MHz, $CDCl_3$) δ 11.142, 8.498, 8.482, 8.189, 8.177, 8.174, 7.845, 7.831, 7.817, 7.628, 7.628, 7.614, 7.599, 7.590, 7.575, 7.560, 7.545, 7.488, 7.471

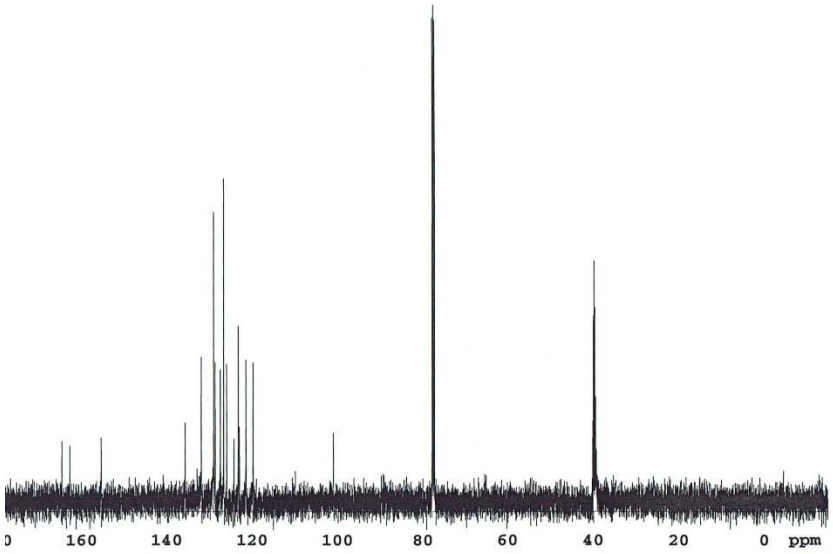

FIG 31 ^{13}CNMR 1,2-HPON (500 MHz, DMSO) δ 155.51, 135.719, 132.023, 129.132, 128.781, 127.576, 126.805, 126.104, 124.387, 123.357, 123.098, 121.557, 119.879, 101.083, 101.068.

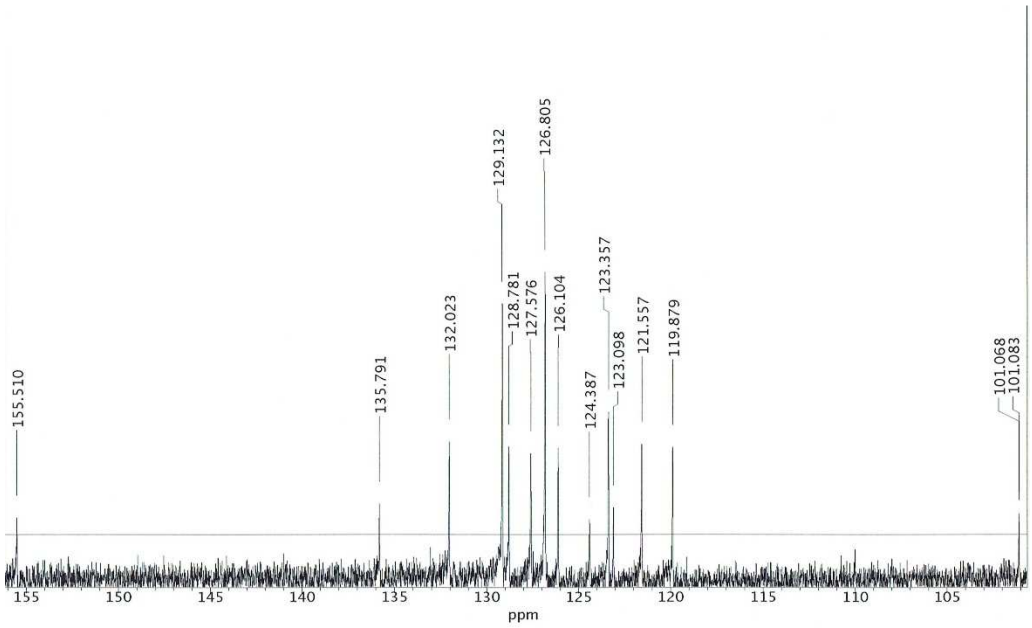

FIG 32 C^{13}NMR 1,2-HPON (500 MHz, DMSO) δ 155.51, 135.719, 132.023, 129.132, 128.781, 127.576, 126.805, 126.104, 124.387, 123.357, 123.098, 121.557, 119.879, 101.083, 101.068.

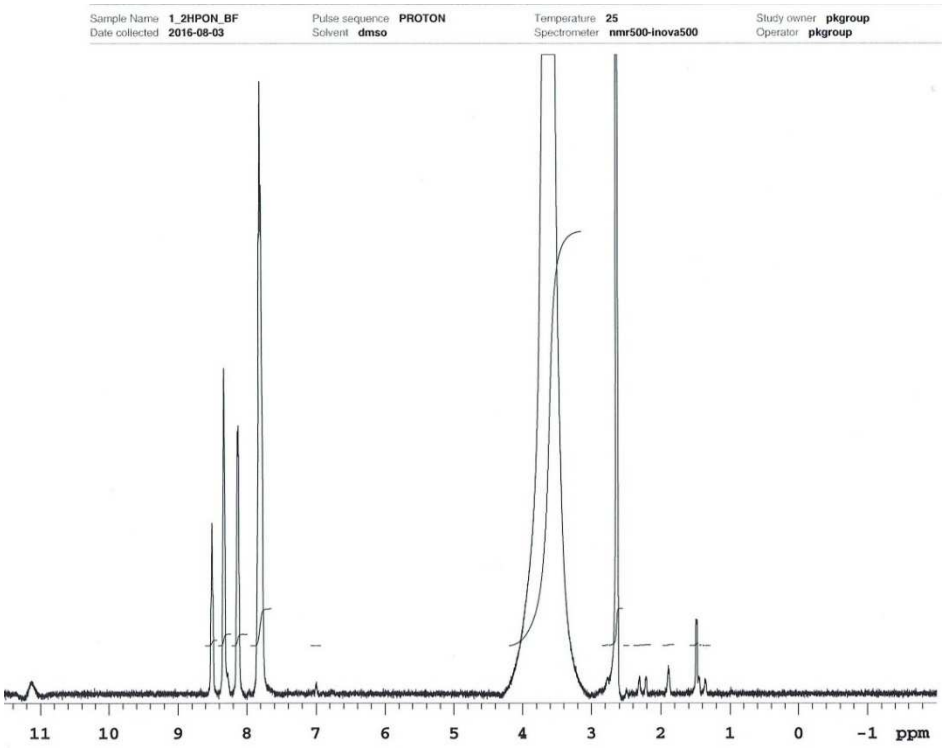

FIG 33 ^{1}HNMR BF_2(1,2-PON)(500 MHz, DMSO) δ 11.264, 8.363, 8.347, 8.189, 8.186, 8.174, 8.170, 7.992, 7.979, 7.975, 7.964, 7.694, 7.681, 7.667, 7.663, 7.648, 7.630, 7.627, 7.616.

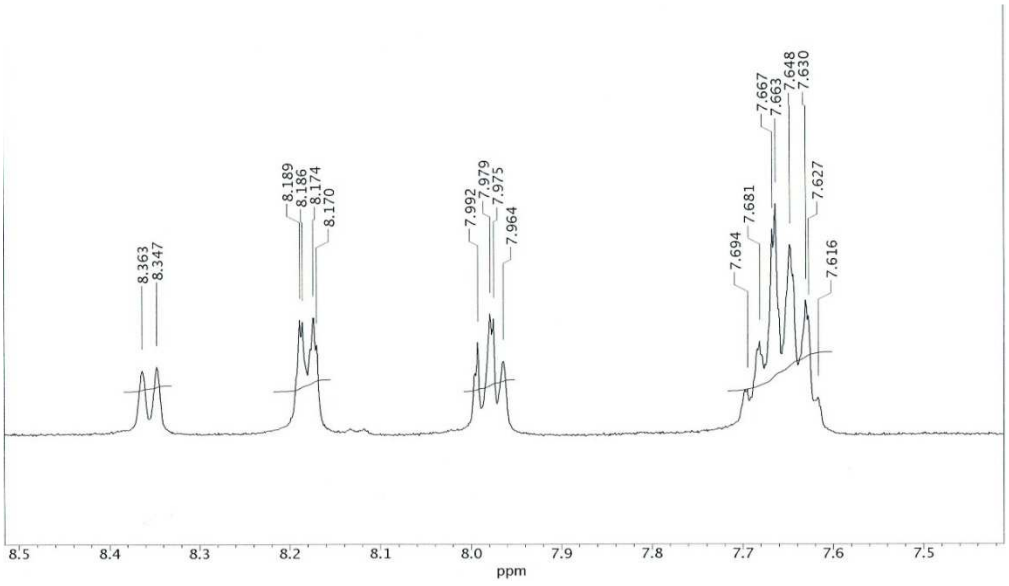

FIG 34 ^{1}HNMR BF_2(1,2-PON)(500 MHz, DMSO) δ 11.264. 8.363, 8.347, 8.189, 8.186, 8.174, 8.170, 7.992, 7.979, 7.975, 7.964, 7.694, 7.681, 7.667, 7.663, 7.648, 7.630, 7.627, 7.616.

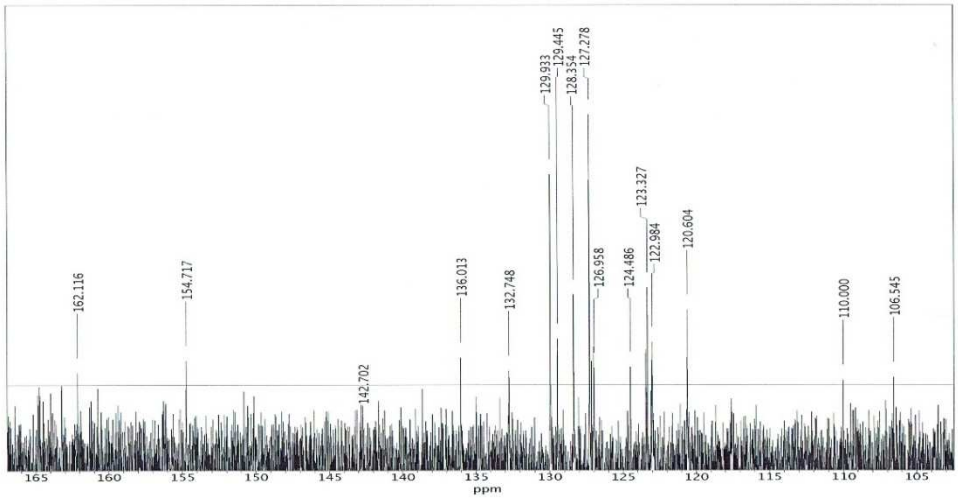

FIG 35 ^{13}CNMR BF_2(1,2-PON)(500 MHz, DMSO) δ 164.817, 163.245, 154.740, 136.043, 132.755, 129.956, 129.460, 128.377, 127.309, 126.996, 124.517, 123.479, 123.357, 123.045, 120.611, 102.380

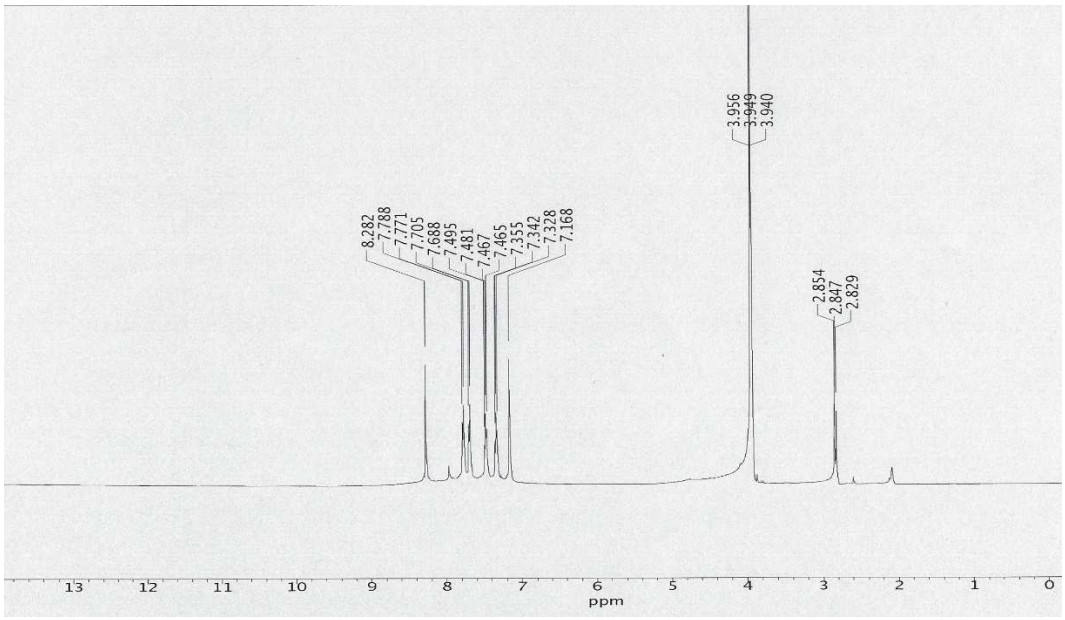

FIG 36 [1]HNMR Methyl 3-Methoxy-2-Naphthoate (500 MHz, $CDCl_3$) δ8.282, 7.788, 7.771, 7.705, 7.688, 7.495, 7.481, 7.467, 7.465, 7.355, 7.342, 7.328, 7.168, 3.956, 3.949, 3.940, 2.854, 2.847, 2.829

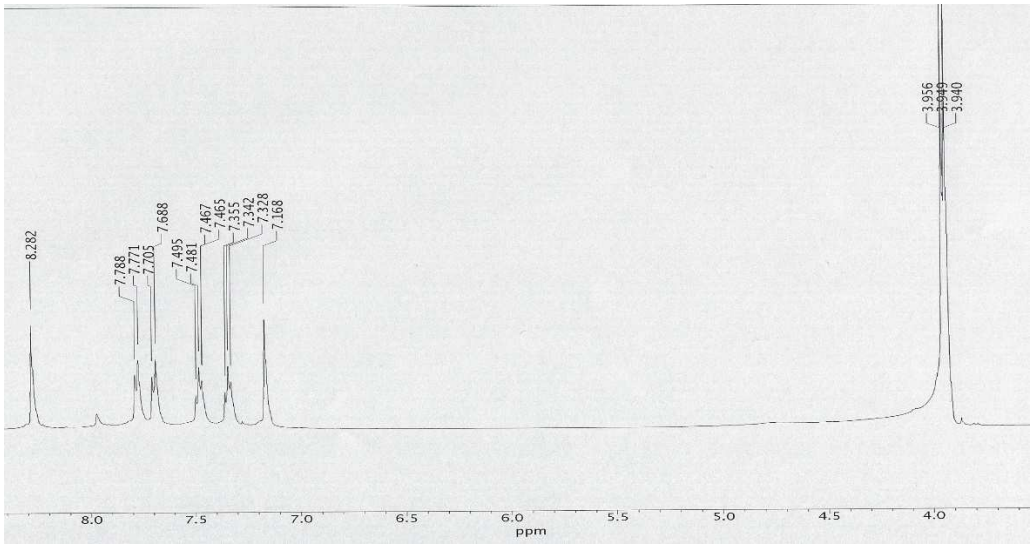

FIG 37 [1]HNMR Methyl 3-Methoxy-2-Naphthoate (500 MHz, $CDCl_3$) δ 8.282, 7.788, 7.771, 7.705, 7.688, 7.495, 7.481, 7.467, 7.465, 7.355, 7.342, 7.328, 7.168, 3.956, 3.949, 3.940, 2.854, 2.847, 2.829

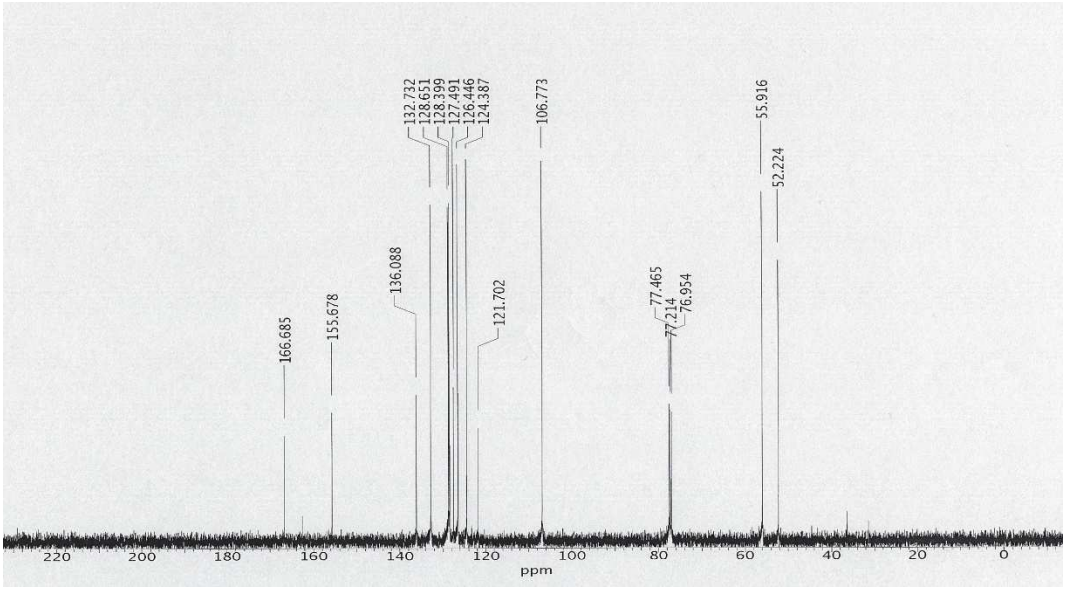

FIG 38 ^{13}CNMR Methyl 3-Methoxy-2-Naphthoate (500 MHz, $CDCl_3$) δ 166.685, 155.678, 136.088, 132.732, 128.651, 128.399, 127.491, 126.446, 124.387, 121.702, 106.773, 55.916, 52.224

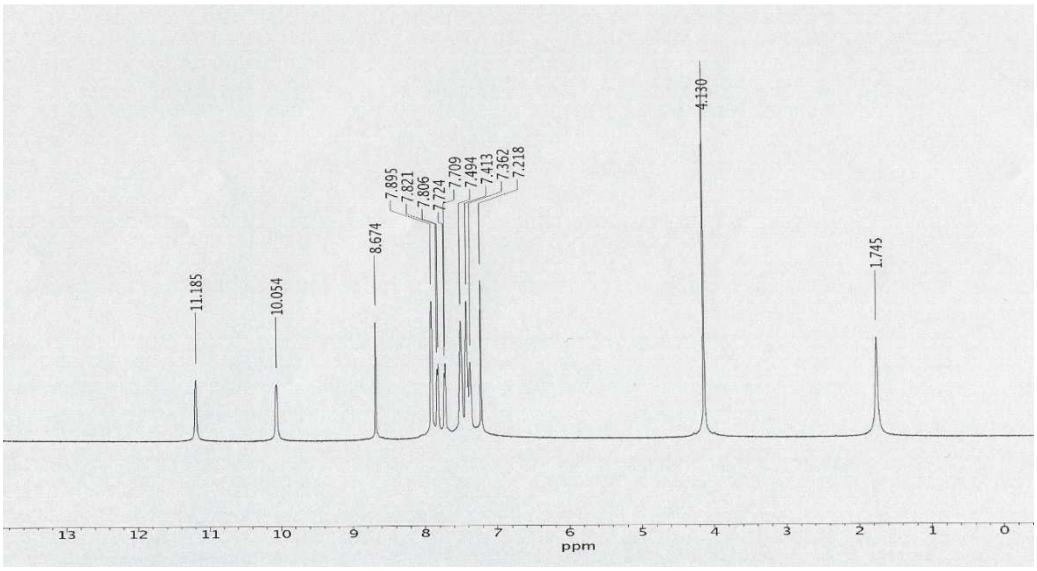

FIG 39 ^{1}HNMR *N'*-Benzoyl-3-Methoxy-2-Naphthohydrazide (500 MHz, CDCl3) δ 11.185, 10.054, 8.674, 7.895, 7.821, 7.806, 7.724, 7.709, 7.494, 7.413, 7.362, 7.218, 4.130

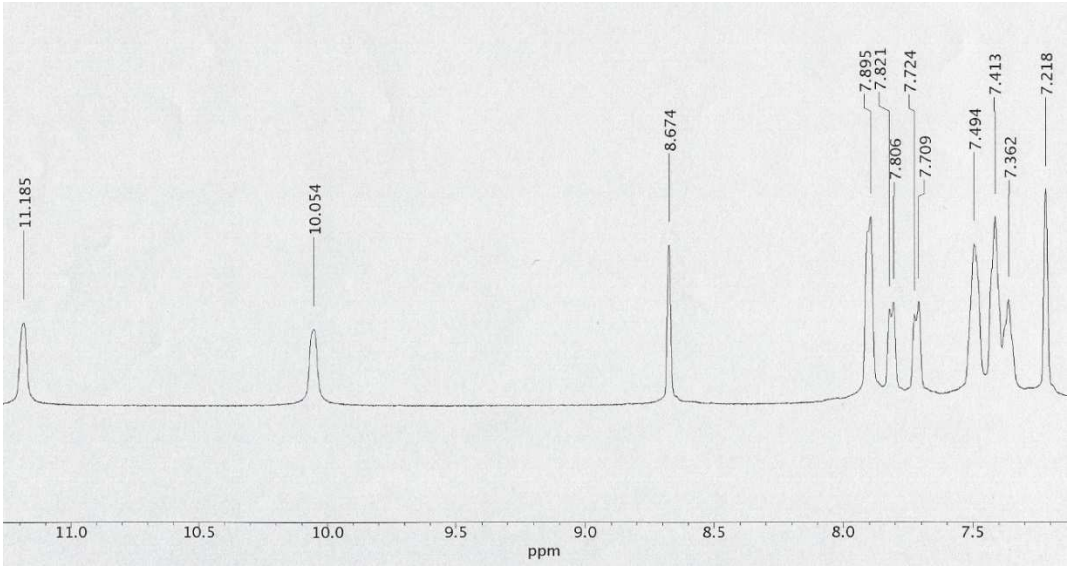

FIG 40 [1]HNMR *N'*-Benzoyl-3-Methoxy-2-Naphthohydrazide (500 MHz, CDCl3) δ 11.185, 10.054, 8.674, 7.895, 7.821, 7.806, 7.724, 7.709, 7.494, 7.413, 7.362, 7.218, 4.130

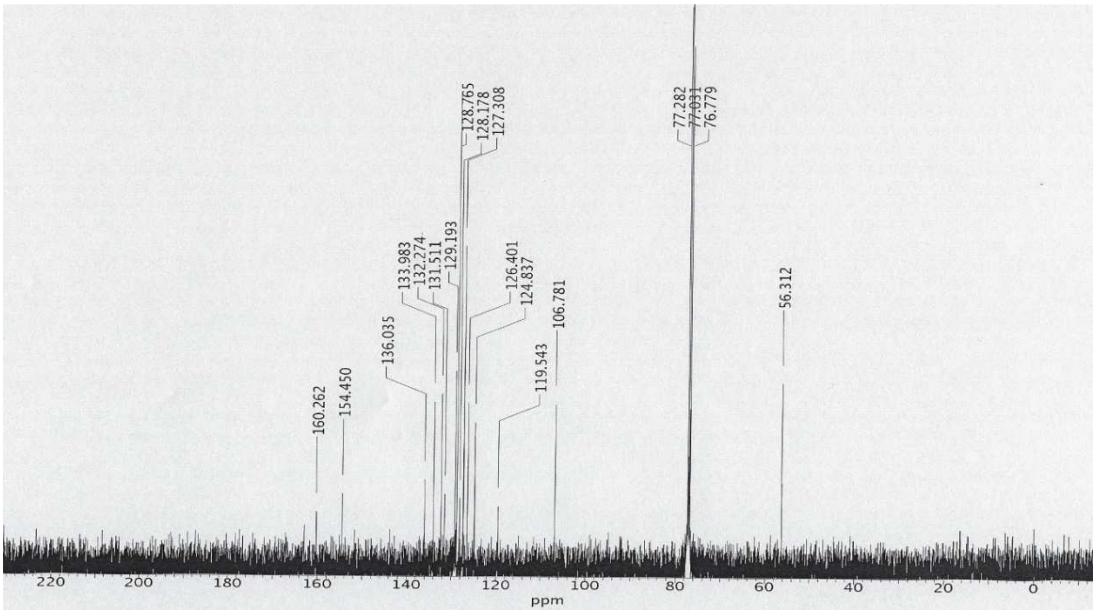

FIG 41 [13]CNMR *N'*-Benzoyl-3-Methoxy-2-Naphthohydrazide (500 MHz, CDCl3) δ 160.262, 154.450, 136.035, 133.983, 132.274, 131.511, 129.193, 128.765, 128.178, 127.308, 126.401, 124.837, 119.543, 106.781, 56.312

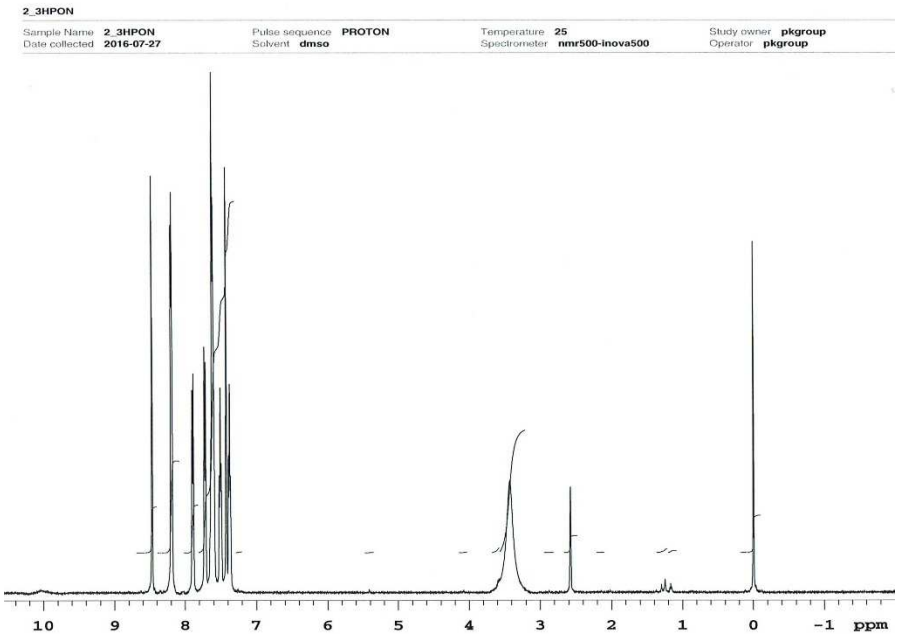

FIG 42 [1]HNMR 2,3 HPON (500 MHz, DMSO) δ aromatic multiplet peaks ranging 8.46-7.36

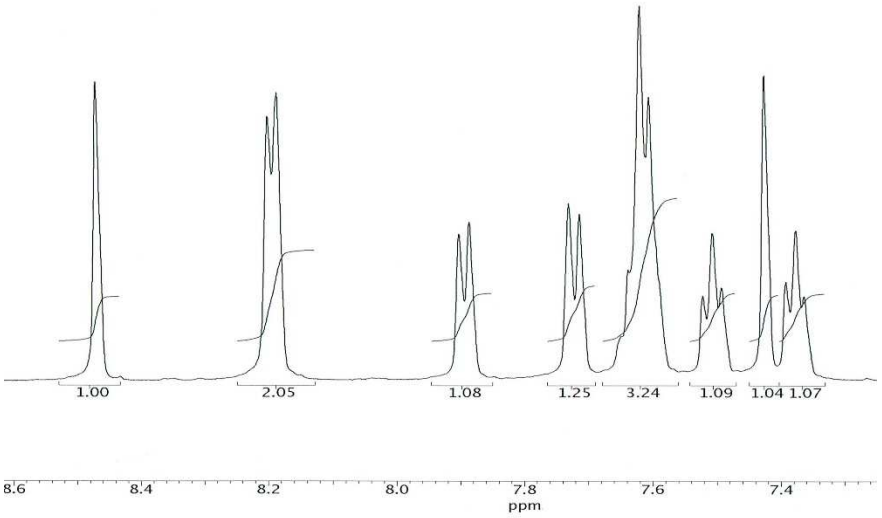

FIG 43 1HNMR 2,3 HPON (500 MHz, DMSO) δ aromatic multiplet peaks ranging 8.46-7.36

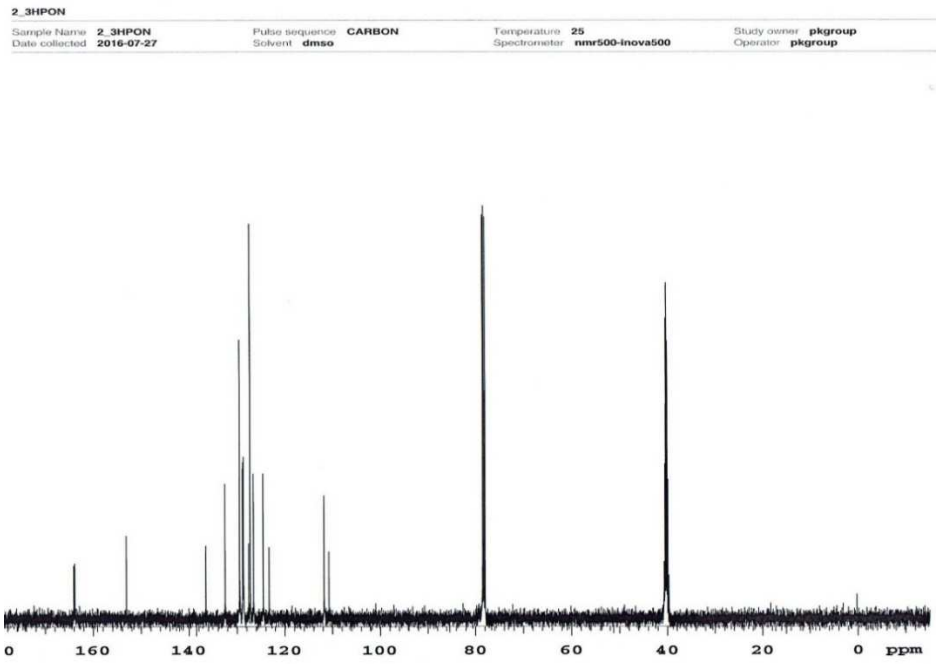

FIG 44 ^{13}CNMR 2,3 HPON (500 MHz, DMSO) δ 64.023, 163.825, 153.100, 136.485, 132.465, 129.437, 128.819, 128.728, 128.613, 127.507, 127.217, 126.546, 124.502, 123.266, 111.755, 110.733

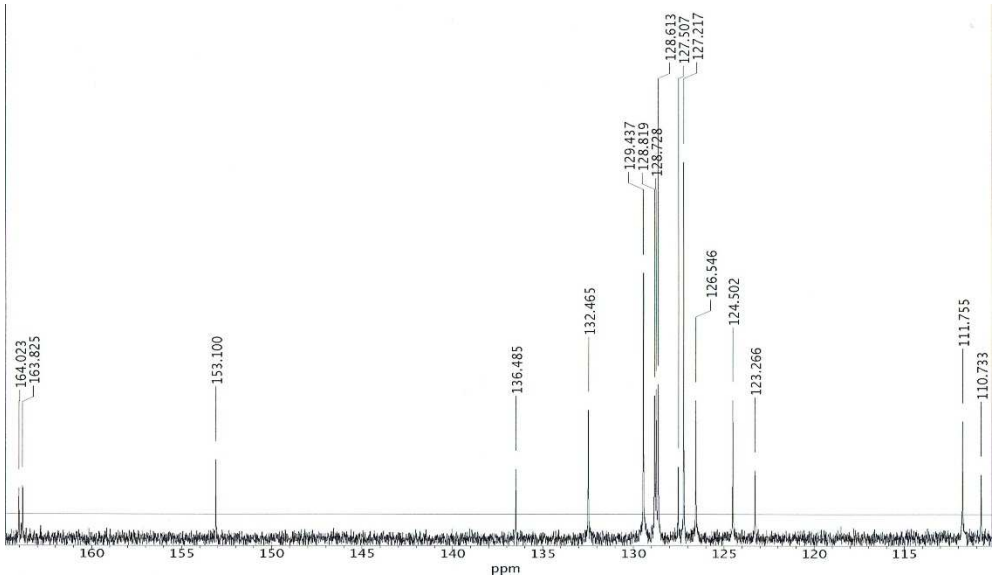

FIG 45 ^{13}CNMR 2,3 HPON (500 MHz, DMSO) δ 64.023, 163.825, 153.100, 136.485, 132.465, 129.437, 128.819, 128.728, 128.613, 127.507, 127.217, 126.546, 124.502, 123.266, 111.755, 110.733

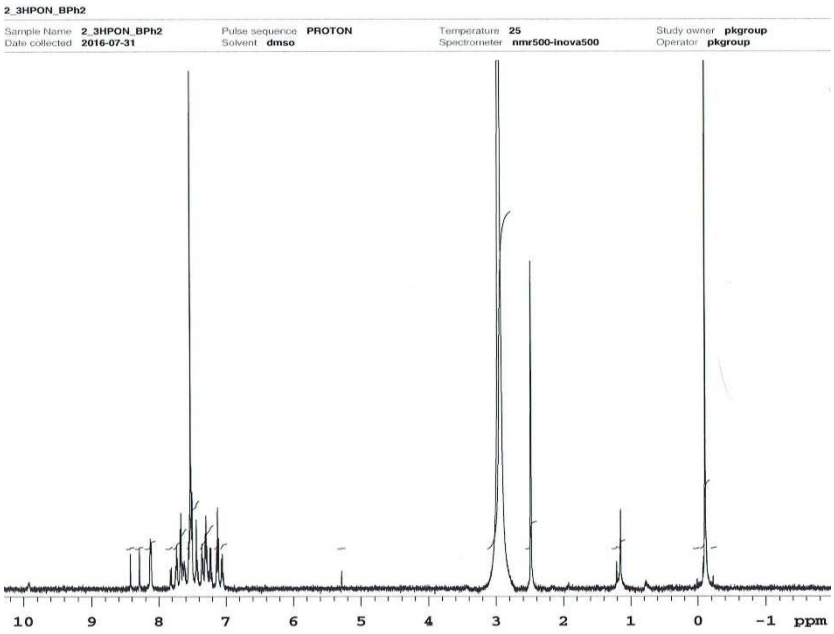

FIG 46 1HNMR 2,3 BPH2(PON) (500 MHz, DMSO) δ 9.920, 8.423, 8.288, 8.127, 8.119, 8.114, 7.831, 7.813, 7.751, 7.736, 7.724, 7.684, 7.670, 7.684, 7.623, 7.60, 7.648, 7.623, 7.600, 7.557, 7.530, 7.527, 7.519, 7.503, 7.442, 7.361, 7.340, 7.312, 7.300, 7.283, 7.256, 7.239, 7.227, 7.211, 7.142, 7.127, 7.113, 7.111, 7.069, 7.057

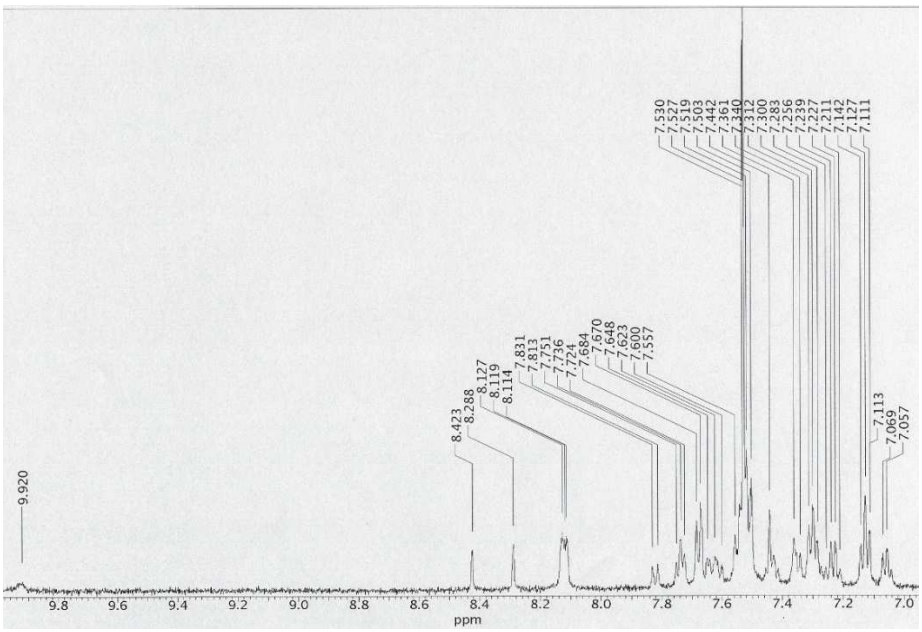

FIG 47 1HNMR 2,3 BPH2(PON) (500 MHz, DMSO) δ 9.920, 8.423, 8.288, 8.127, 8.119, 8.114, 7.831, 7.813, 7.751, 7.736, 7.724, 7.684, 7.670, 7.684, 7.623, 7.60, 7.648, 7.623, 7.600, 7.557, 7.530, 7.527, 7.519, 7.503, 7.442, 7.361, 7.340, 7.312, 7.300, 7.283, 7.256, 7.239, 7.227, 7.211, 7.142, 7.127, 7.113, 7.111, 7.069, 7.057

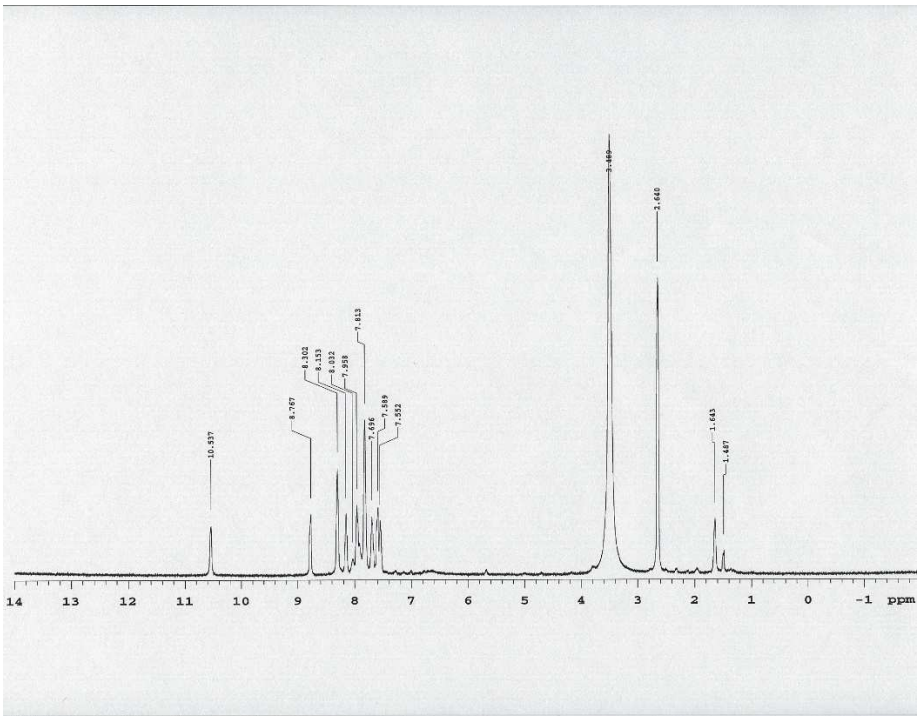

FIG 48 1HNMR 2,3 BF2(PON) (500 MHz, DMSO) δ 10.537, 8.767, 8.302, 8.153, 8.032, 7.958, 7.813, 7.696, 7.589, 7.552, 3.489, 2.640, 1.643, 1.487

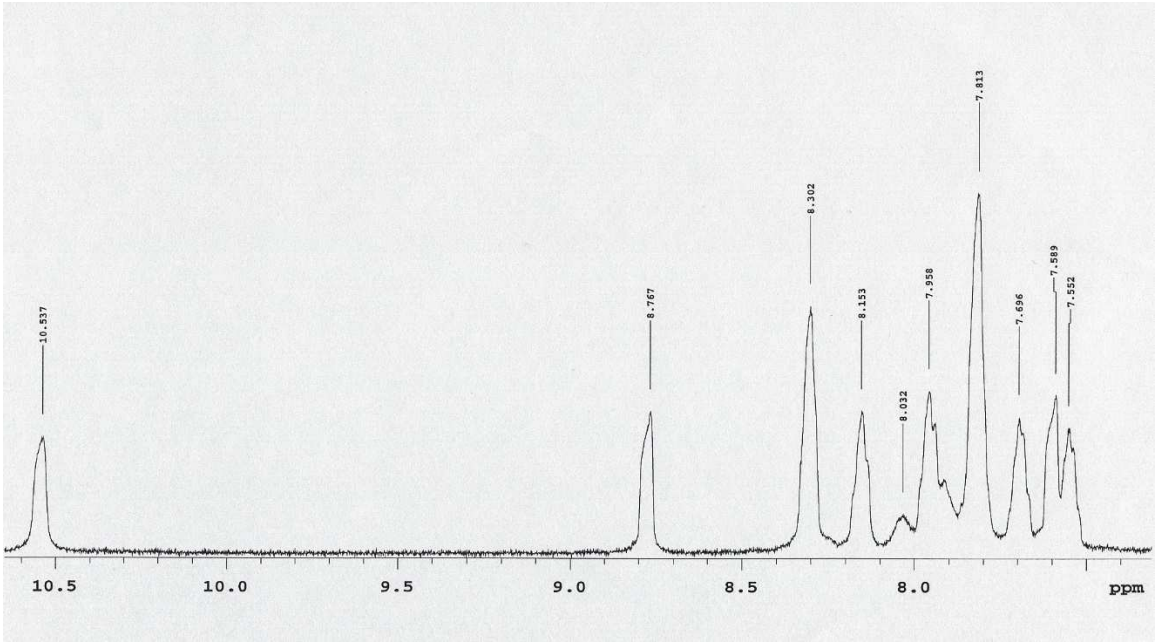

FIG 49 1HNMR 2,3 BF2(PON) (500 MHz, DMSO) δ 10.537, 8.767, 8.302, 8.153, 8.032, 7.958, 7.813, 7.696, 7.589, 7.552, 3.489, 2.640, 1.643, 1.487

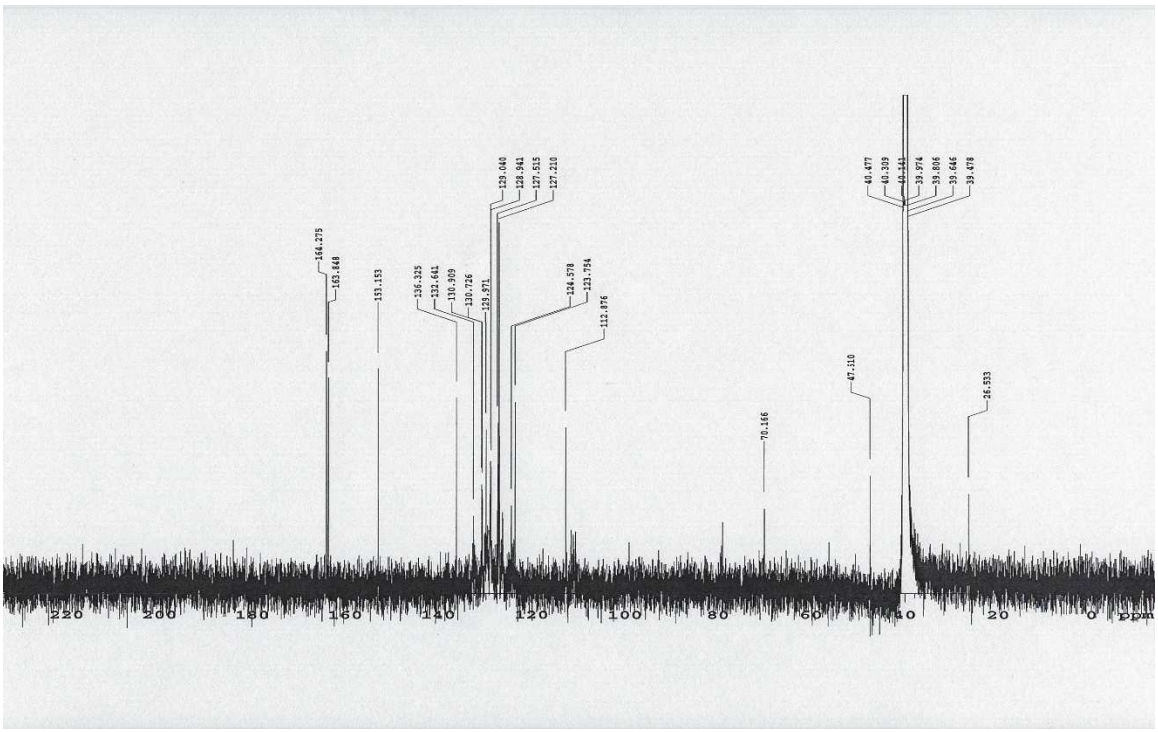

FIG 50 ^{13}CNMR 2,3 BF2(PON) (500 MHz, DMSO) δ 164.275, 163.848, 153.153, 136.325, 132.641, 130.909, 130.726, 129.971, 129.040, 128.941, 127.515, 127.210, 124.578, 123.754, 112.876, 70.166, 47.510, 26.533

LCMS Spectroscopy

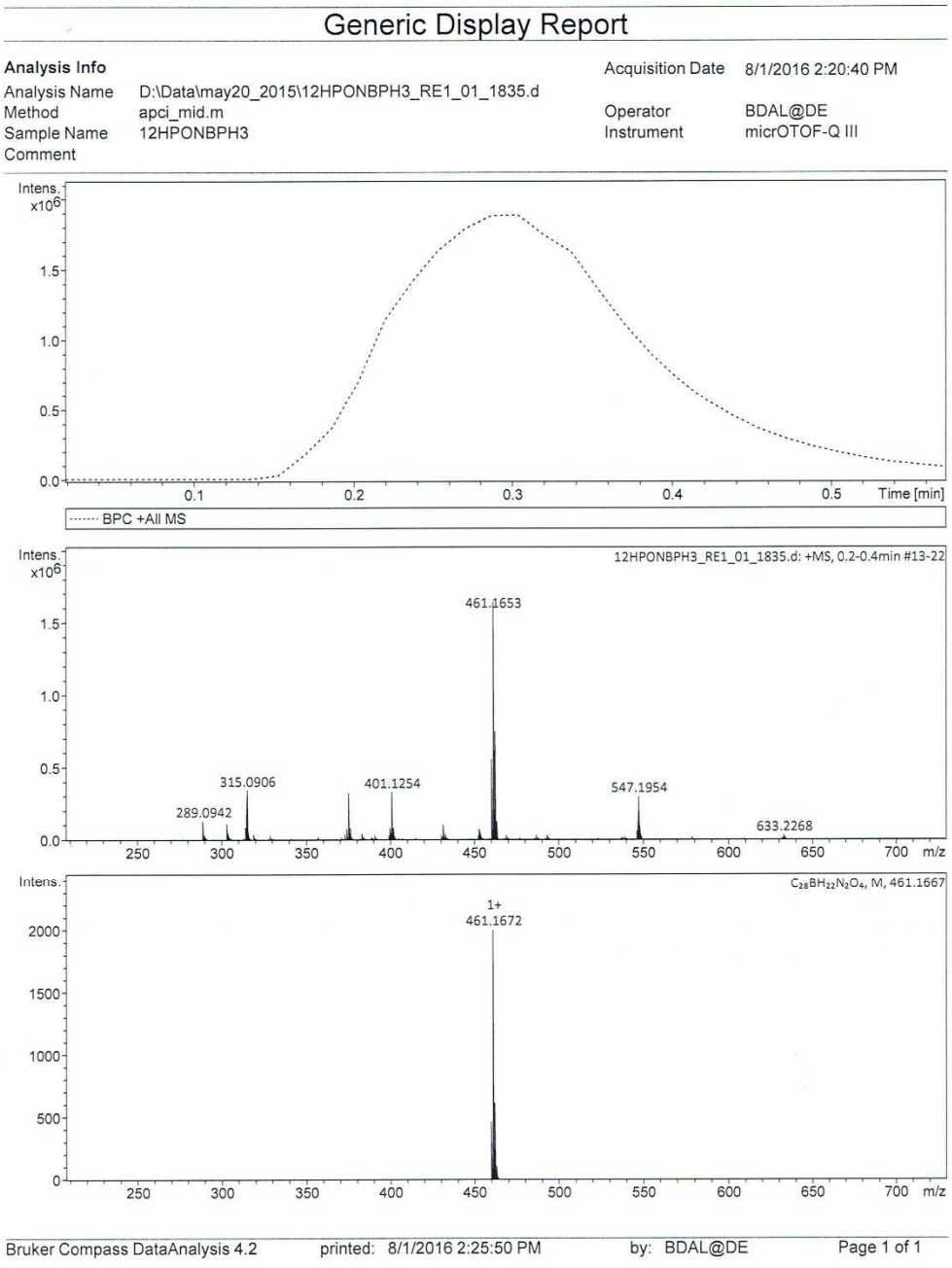

FIG 51 LCMS BPh_2(1,2-PON)

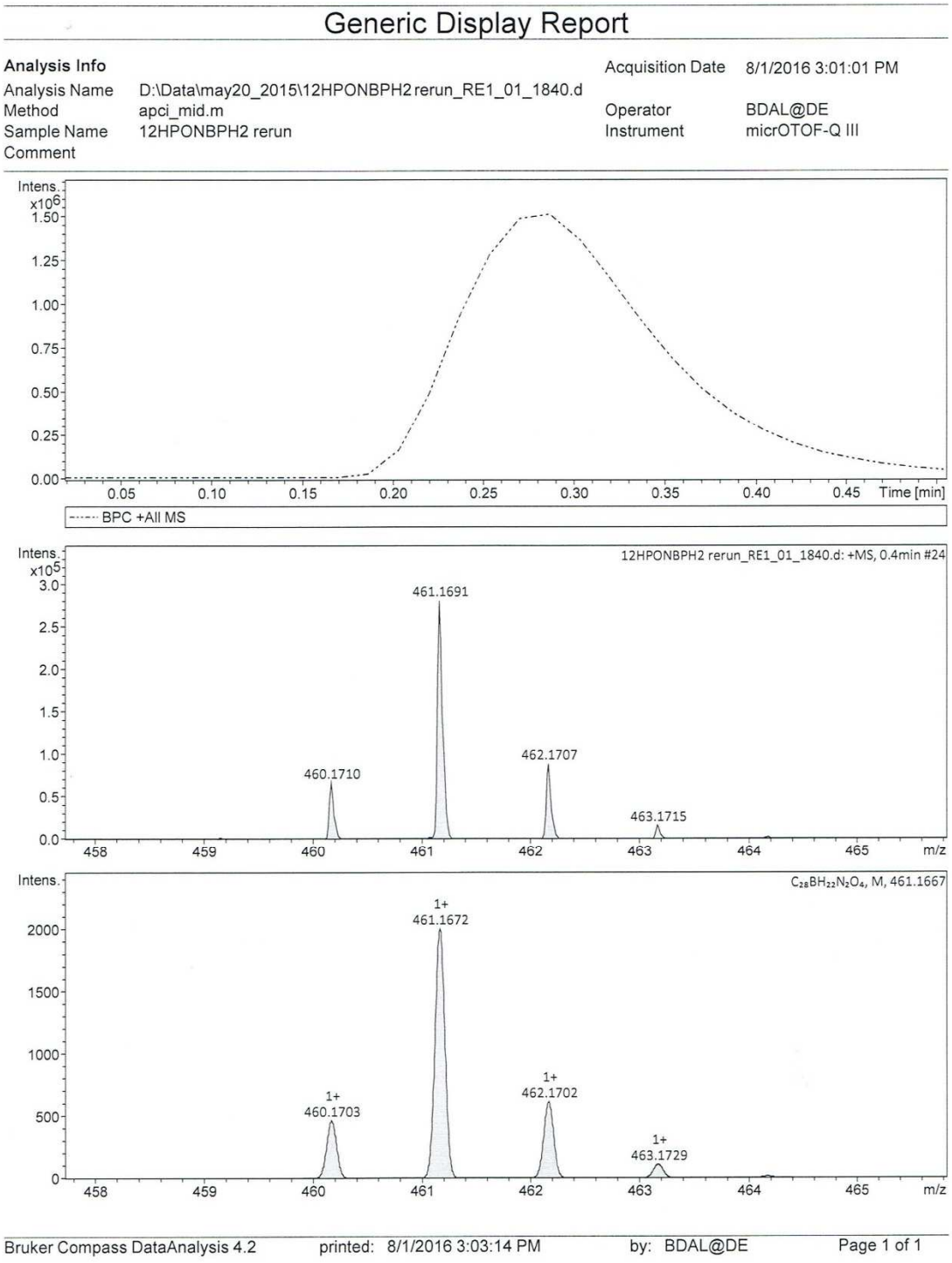

FIG 52 LCMS BPh_2(1,2-PON)

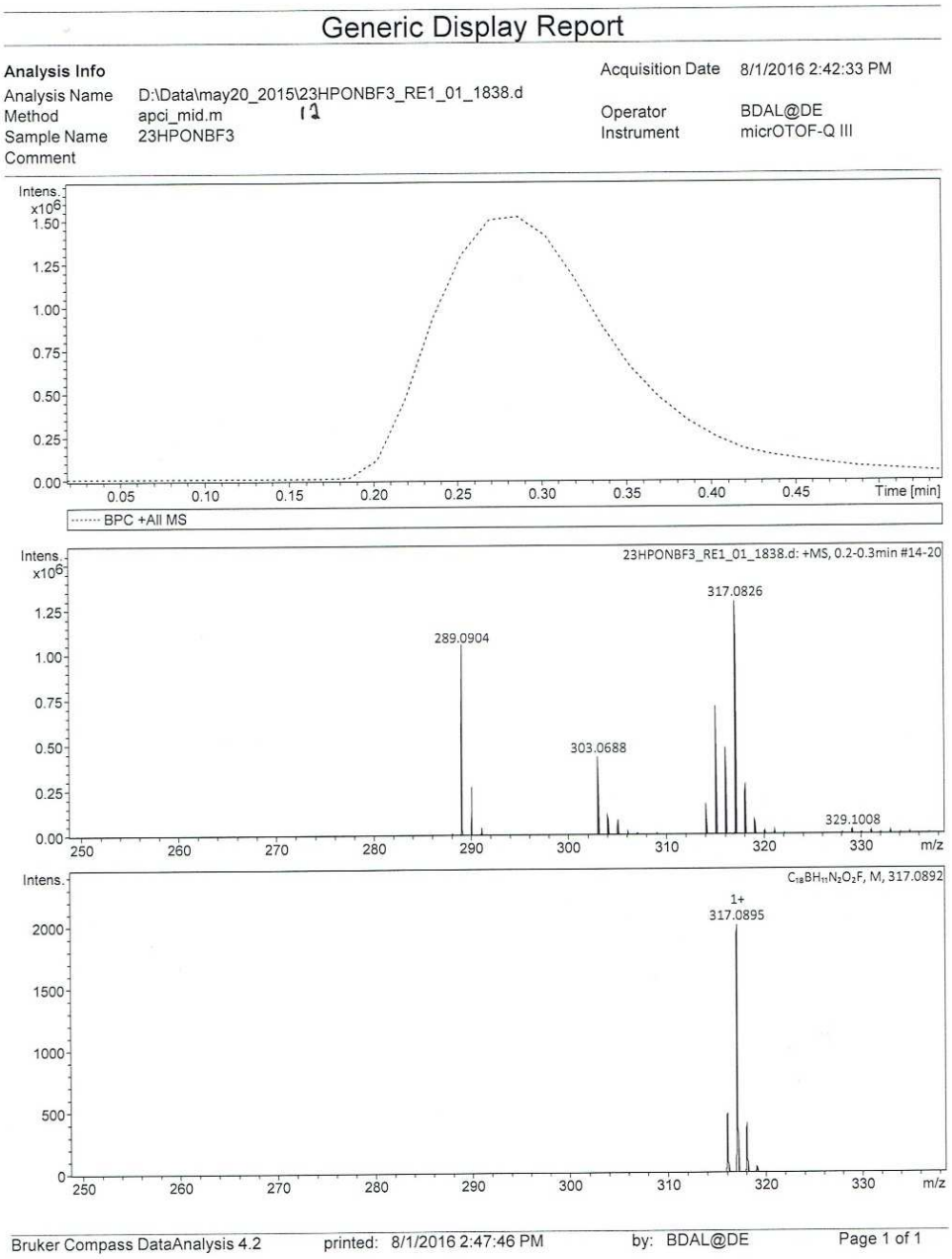

FIG 53 LCMS BF_2(1,2-PON)

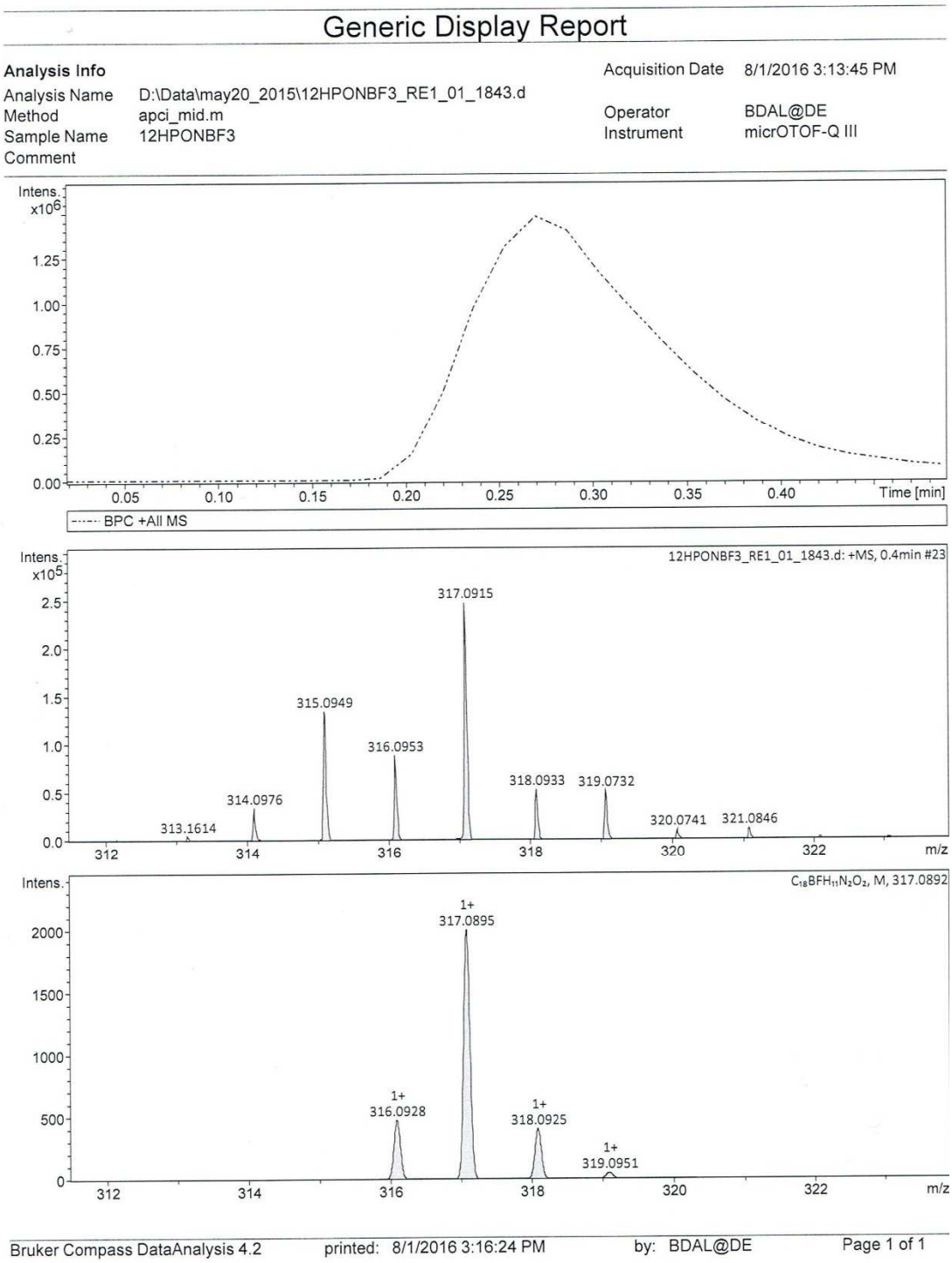

FIG 54 LCMS BF_2(1,2-PON)

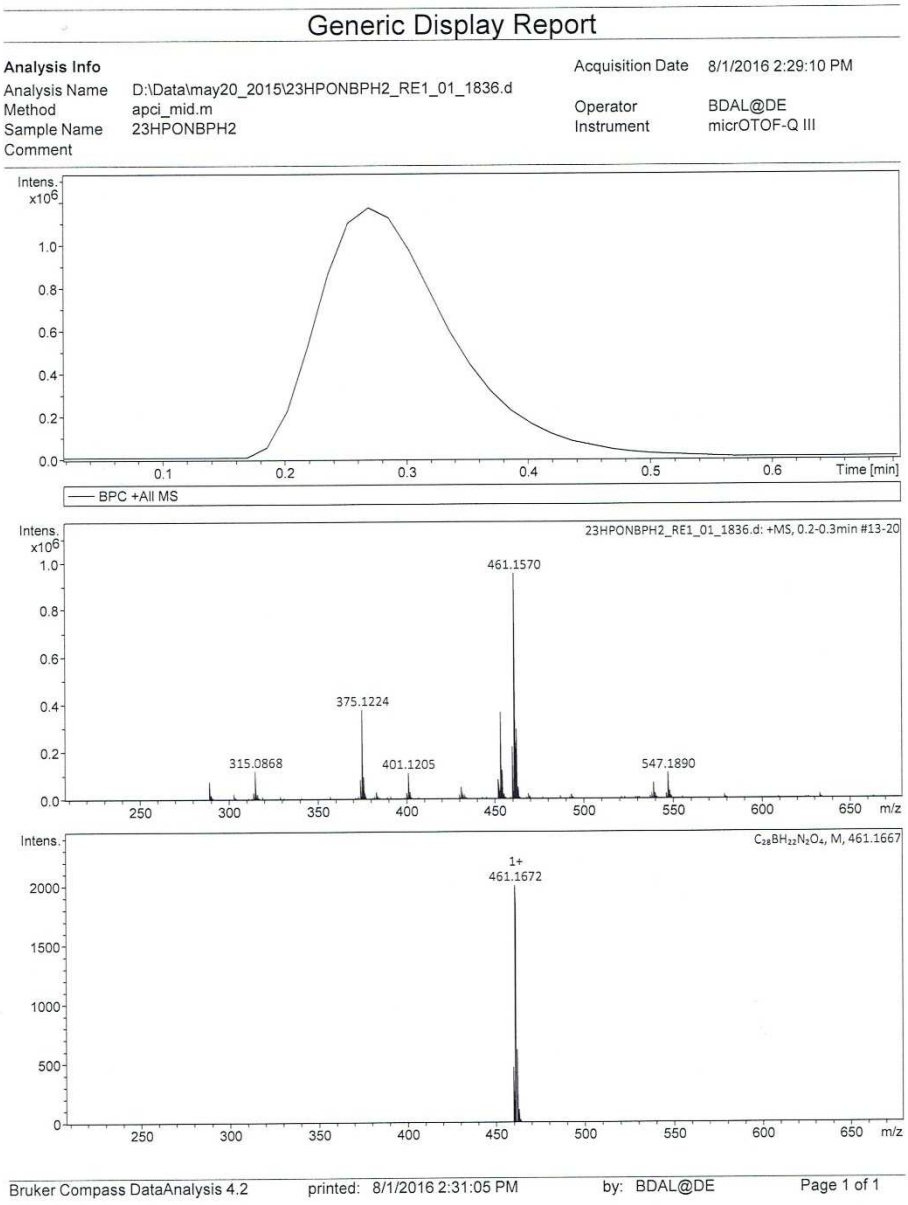

FIG 55 LCMS BPh_2(2,3-PON)

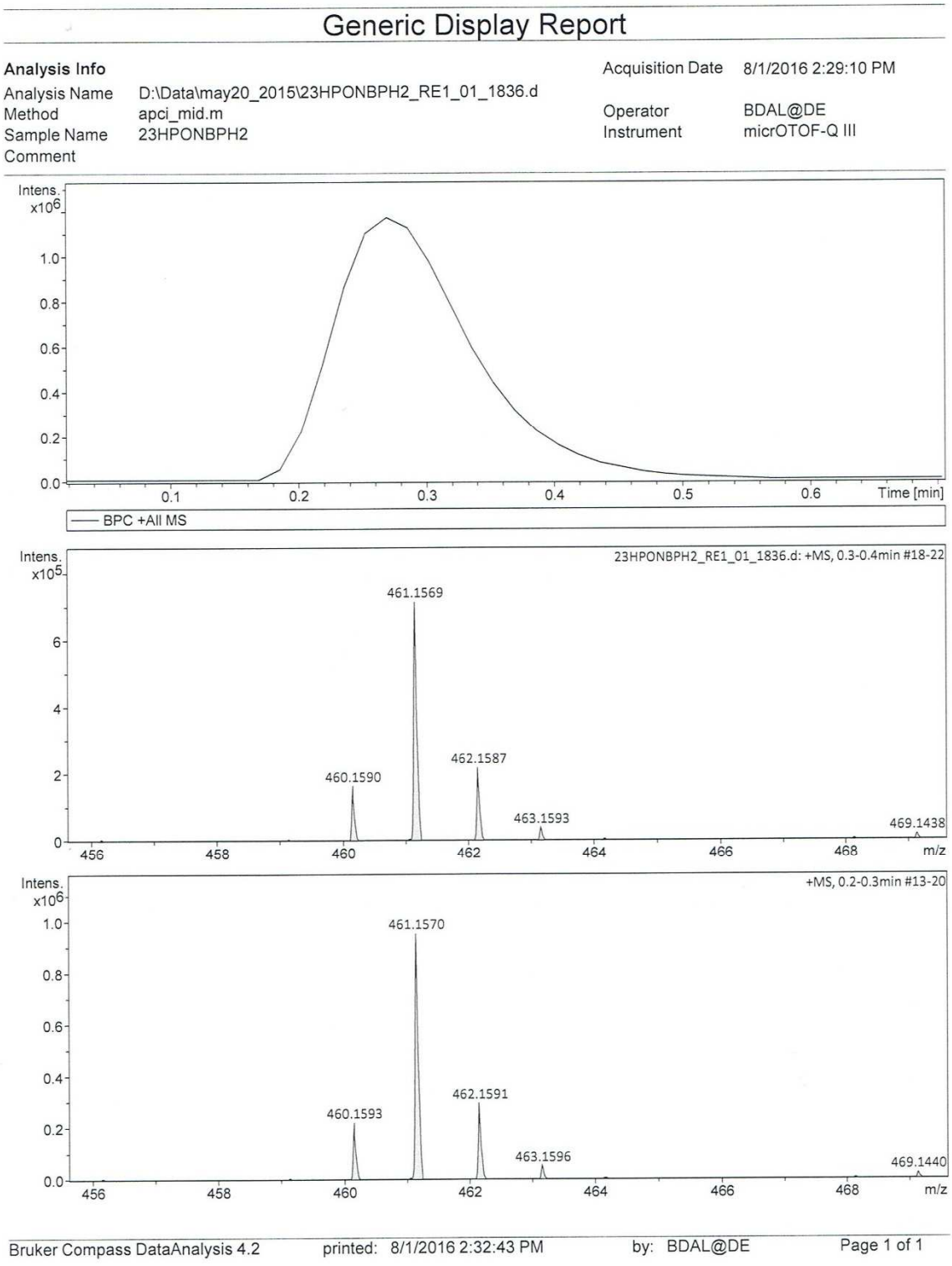

FIG 56 LCMS BPh_2(2,3-PON)

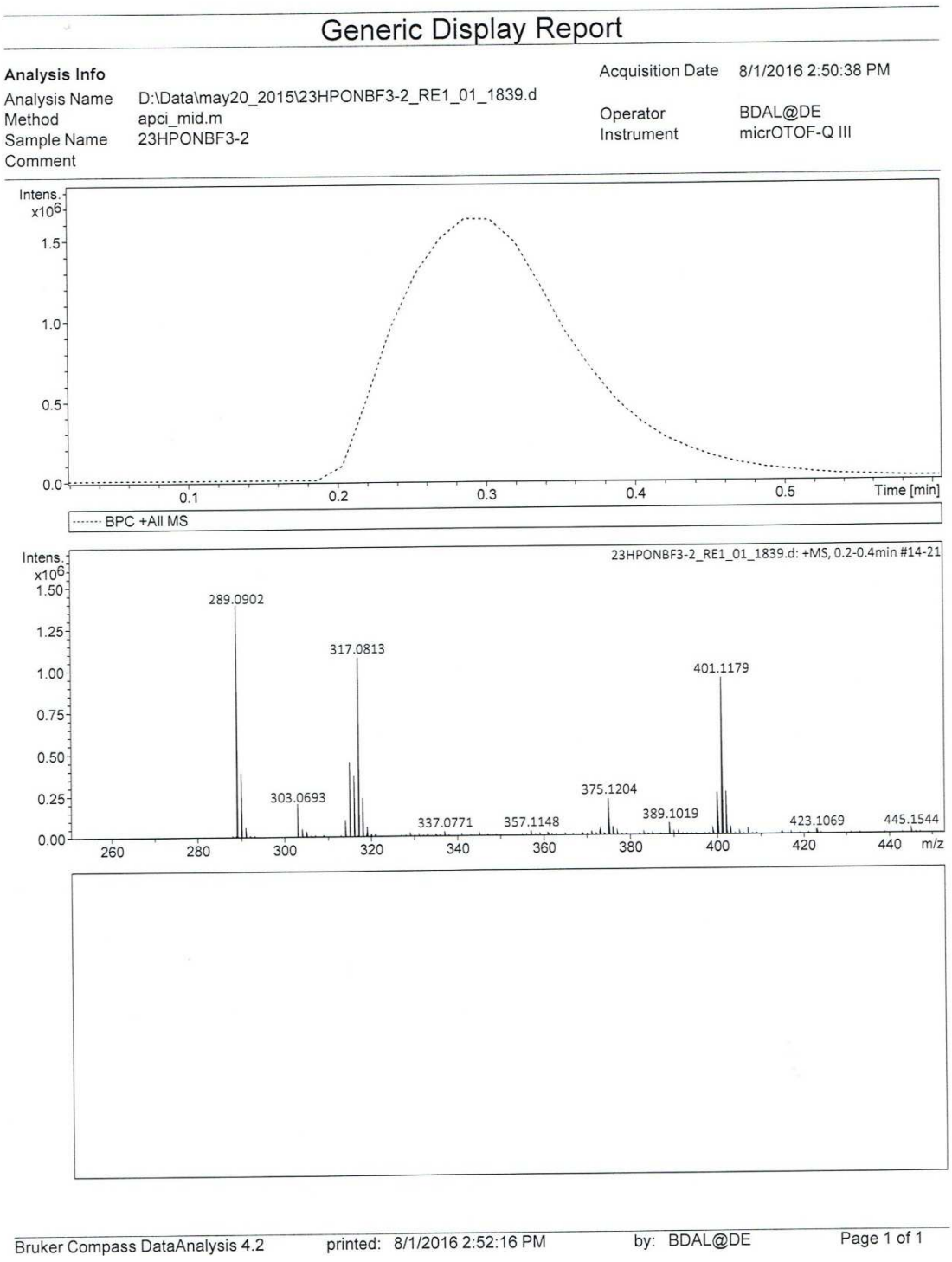

FIG 57 LCMS BF_2(2,3-PON)

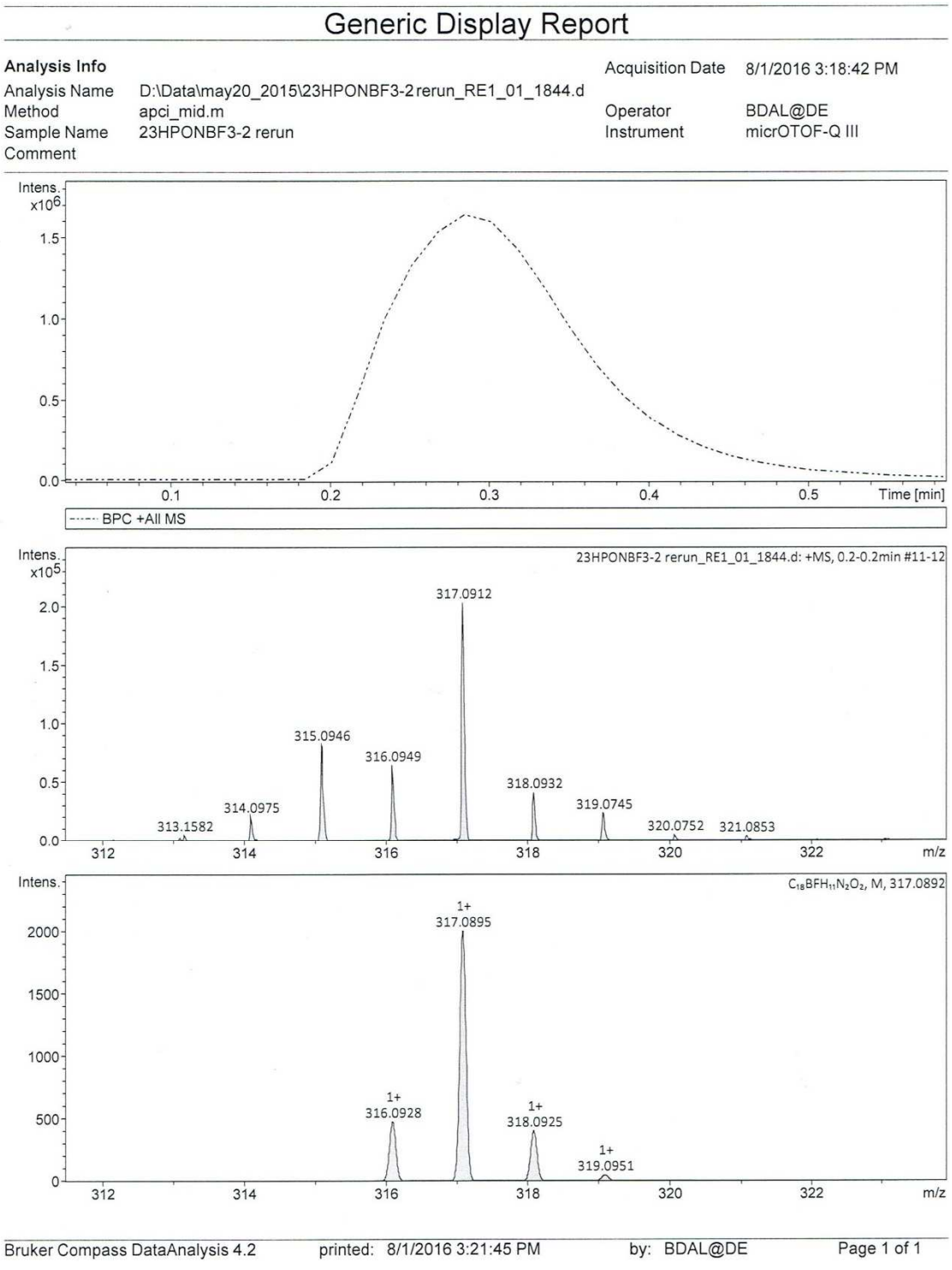

FIG 58 LCMS BF_2(2,3-PON)